

**Annual Review**  
**2014**

**Molecular Photoscience**  
**Research Center**

**Kobe University**

## Preface

This annual review provides a summary of the research activity of Molecular Photoscience Research Center for the 2014 fiscal year. We are further promoting advanced research and international collaboration on molecular photoscience and related topics. Any constructive comments and questions, and any suggestion for collaboration research are welcome.

MPRC belongs to Cluster of Centers of Organization of Advanced Science and Technology Kobe University. In this year OAST selected 19 Core Research Teams from five Graduate Schools in the fields of natural science (Science, Engineering, System Information, Agricultural Science, and Maritime Sciences), and each team has started its research activity. Some researchers of MPRC also participate in these Core Research Teams to further advanced and interdisciplinary science by collaborating with members in the Teams.

March, 2015

Keisuke Tominaga  
Director of Molecular Photoscience Research Center,  
Kobe University



## **Contents**

Members	4
Research Activities	
Laser Molecular Photoscience Laboratory	5
Ultrafast Photoscience Laboratory	16
Coherent Photoscience Laboratory	31
Original Papers	39
Invited Talks	42
Presentation at Conferences (International and domestic)	44
Presentation by Graduate Students and Postdocs	46
Books	51
Other Publications	52
Lectures to Public	53
Awards	54
Conference Organization	55
Molecular Photoscience Seminar	56

## Members

Keisuke Tominaga                      Director  
Hitoshi Ohta                              Vice-Director

Yuma Kato                                Assistant  
Keiko Katayama                        Assistant (~ June 2014)  
Megumi Soma                             Assistant  
Takako Miyazaki                        Assistant (August 2014 ~)

### Laser Molecular Photoscience Laboratory

Akihide Wada                            Professor  
Shunji Kasahara                        Associate Professor  
Neeraj Kumar Joshi                     Kobe University Visiting Research Fellow (~ January 2015)

### Ultrafast Photoscience Laboratory

Keisuke Tominaga                      Professor  
Seiji Akimoto                            Associate Professor  
Kaoru Ohta                                Research Associate Professor  
Naoki Yamamoto                        Postdoctoral Fellow (~ June 2014)  
Minako Kondo                            JSPS Postdoctoral Fellow (~ September 2014)  
Feng Zhang                                Postdoctoral Fellow  
Jessica Afalla                             Kobe University Visiting Research Fellow (March 2015 ~)

### Coherent Photoscience Laboratory

Hitoshi Ohta                              Professor  
Susumu Okubo                            Assistant Professor  
Keigo Hijii                                Postdoctoral Fellow  
Alexey Alfonsov                         Kobe University Visiting Research Fellow

## Research Activity

### I. Laser Molecular Photoscience Laboratory

#### I-A. OPTICAL CONTROL OF PHOTO-REACTION NETWORK

Chemical reaction induced by photo-irradiation consists of several reaction pathways such as multiphoton/multistep reaction paths subsequent to photo-excitation to S1 state, even if one-photon reaction is a major pathways. In order to understand and control such branched reaction pathways called photo-reaction network, in addition to the knowledge of each reaction oaths, knowledge of correlation and balance between paths is necessary in addition to the information about each reaction path. The goal of this study is to understand and control the whole photo-reaction network. The initial step for understanding a natural phenomenon is to observe it carefully. Recent developments in laser technology have made it possible to observe the structure and the dynamics of atoms and molecules at high energy resolutions and/or high time resolutions. When the observation has been done as much as possible, scientific research should then progress to the next stage, namely interpretation of the reaction mechanism and construction of the model of reaction mechanism.

One of the method to confirm the validity of constructed model is to examine the response of the photo-reaction network to shaped pulse on the basis of the model. In addition, pulse-shaping techniques have great potential to contribute to the progress of theoretical and experimental studies concerned with optically controlling the dynamics of molecular systems. These techniques are particularly pertinent for research into polyatomic molecules or molecules in condensed phases. However, the pulse-shaping method usually needs a huge number of parameters such as amplitude and phase on each frequency included in the shaped pulse. Then reduction of the number of parameters is an important issue. Two-pulse correlation technique is a kind of the simplest pulse-shaping techniques, in which a variable parameter is pulse interval. This technique is an effective tool to investigate and control the photo-reaction network. In this study, the reaction mechanism and control method of photo-reaction network was investigated by time-resolved measurements and pulse-shaping technique such as two-pulse correlation.

#### **On the Branching Ratio of Photoisomerization in 4-Aminoazobenzene**

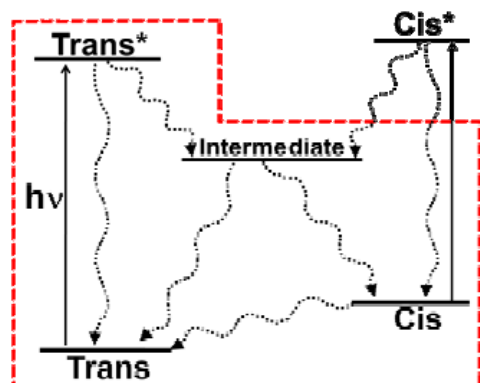
**Neeraj K. Joshi, Masanori Fuyuki, and Akihide Wada**

*(Annual Meeting of Japan Society for Molecular Science, 2014)*

Study of the reaction path ways and the relaxation processes of photoexcited molecules are fundamental part of investigation for any photoinduced reaction and such information yields

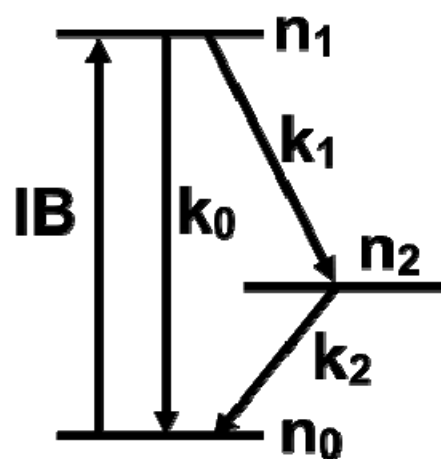
an opportunity to control the photochemical reactions. For that purpose, photoisomerization reaction in azobenezne (AB) and its derivatives has been well studied in which trans-to-cis isomerization reaction is initiated by the irradiation of UV-visible light. On the other hand, cis-to-trans thermal isomerization spontaneously takes place in the dark owing to the thermodynamic stability of the trans isomer<sup>1</sup>, and our recent study on 4-aminoazobenzene (AAB) has revealed that the

mechanism and the kinetics of thermal isomerization of AAB strongly depends on the polarity of the medium and is independent of the viscosity of the medium.



Scheme 1

In this study, as a part of our investigation on the photoreaction network of AAB, we focused on the branching ratio of photoisomerization, namely the production ratio between cis-isomer and trans-isomer from photoexcited state of trans-isomer. The most significant aspect of the study is that the method for estimating the branching ratio does not require the ultrafast time resolved measurement but a simplistic approach has been employed. Briefly, the population at photostationary state (cis isomer) is measured as function of pumping rate, and the observed results are discussed quantitatively based on the three-level model (described below) which provide some insight on the mechanism of photoisomerization in viscous medium.



Scheme 2

In general, for understanding the photoisomerization in azobenzene family schematically, a five level energy diagram (scheme 1) is considered. In our case, photoexcitation of cis-AAB is negligible due to very low absorption cross-section for pump 405 nm. Therefore, the effect of excited state of cis-isomer can be neglected and the five level system can be modified to four level system as indicated by red broken line in the scheme 1. Furthermore, under the definition of branching ratio as described above, the four level system can be simplified to three level system as shown in scheme 2. In scheme 2,  $n_0$  corresponds to the population of trans-form in the ground state under photostationary state,  $n_1$  represents the sum of the population of trans-form in the excited state and population in the intermediate state. The population of cis produced by photoisomerization of trans is denoted by  $n_2$ . The rate constants,  $k_0$  and  $k_1$ , represent the decay rate of those molecules which do not undergo for photoisomerization and the decay rate of those molecules which relax after photoisomerization, respectively. Rate of thermal

cis-to-trans isomerization is shown by  $k_2$ . In our recent study the order of the  $k_2$  in MeOH and EG has been determined<sup>2</sup> as in the order of one. However the rate constant for  $k_0$  and  $k_1$  has also been determined which is much higher<sup>3</sup> (in the order of  $10^{12}$  to  $10^{14}$  s<sup>-1</sup>) than  $k_2$ . Thus the total population ( $N$ ) of the three level system which is sum of  $n_0$ ,  $n_1$ , and  $n_2$ , i.e.,  $N = n_0 + n_1 + n_2$ , can be expressed as  $N \sim n_0 + n_2$ .

Using three level system and above approximation, the branching ratio ( $r$ ) defined as above is equivalent to ratio of  $k_0$  to  $k_1$ . Namely, the branching ratio can be expressed as  $r = k_0/k_1$ . For estimation of branching ratio, the population under photostationary state as function of pumping rate (IB) is calculated by monitoring the bleaching at absorption peak for methanol (MeOH) and ethylene glycol (EG). In the analysis, under steady state condition, it is assumed that number of bleached molecules in level-0 are equal to the number of molecules present at level 2 (scheme 2). The ratio of  $N/n_0$  versus IB is plotted and fitted to the equation as follows;

$$\frac{N}{n_0} = 1 + m \times IB \quad (1)$$

where  $m = 1/(r + 1)k_2$  and  $r = k_0/k_1$ .

Equation (1) is derived from the solution of

differential equation for scheme 2 under steady state condition. For calculating IB, at first, decrease in pump power before and after the sample is noticed and divided by per photon energy (i.e.,  $5 \times 10^{-19}$  J for 405 nm) which is the measure of bleached /excited molecules or absorbed photon per second. Further, by dividing to number of photon absorbed per second by active sample volume, the value of  $IBn_0$  can be obtained. Once the  $IBn_0$  is known and by measuring the  $n_0$ ,  $IB$  can be estimated.

The plot of  $N/n_0$  versus IB is fitted to Eq. 1 gives a slope ( $m$ ) as shown in Fig. 2 and hence branching ratio ( $r$ ) can be estimated based on the value of  $k_2$  reported in our previous report<sup>2</sup>. It is observed that branching ratio is significant different between MeOH and EG. Calculated value of the branching ratio ( $k_0/k_1$ ) for MeOH and EG is 0.9 ( $\pm 0.06$ ) and 0.3 ( $\pm 0.02$ ), respectively. Here it should be mentioned that MeOH and EG have similar polarity but quite different viscosity. Therefore, it seems that in contrast to thermal isomerization, mechanism for photoisomerization for 4-AAB is sensitive to viscosity and photoisomerization mechanism may be different in EG than MeOH. Alternatively, this situation can be better probed by ultrafast transient experiments which are under course of investigation.

## I-B. NEW TECHNIQUE FOR ANALYZING PHOTO-REACTION NETWORK

Photochemical reactions initiated by multiphoton/multistep absorption are essentially different from conventional one-photon photochemical reactions because the character of the populated state depends on the optical order of the excitation process and new photochemical reaction channels are opened through the excitation of reaction intermediates. In this regard, knowledge of the contribution of the

multiphoton/multistep process to photochemical reactions is necessary to exploit new photochemical reaction pathways, and the multiphoton process is expected to play a vital role in the optical control of chemical reactions. In this study, Fourier transformed two-dimensional excitation spectrometer was developed on the basis of the Fabry-Pérot interferometer.

### **Fourier Transform Two-dimensional Fluorescence Excitation Spectrometer (FT-2DFES) by Using Tandem Fabry-Pérot Interferometer**

**Hiroshi Anzai, Neeraj Kumar Joshi, Masanori Fuyuki, Akihide Wada**

*(Rev. Sci. Instr., 2015)*

Inter- and intramolecular interaction processes play an important role in photochemical reactions, and knowledge of those processes is necessary to understand the reaction mechanism and the reaction path. One of the methods to investigate inter- and intramolecular interactions is two-dimensional (2D) spectroscopy and the 2D observation has several advantages: simplification of complex spectra consisting of many overlapping peaks, clarification of correlation between the observed spectral peaks, and establishment of unambiguous assignments based on correlation bands.

In this study, a Fourier transform 2D fluorescence excitation spectrometer (FT-2DFES) shown in Figure 1 was developed. The system has a wide excitation spectral range of 380 nm to 800 nm and an intense excitation power achieved by using a high-power Xe lamp. In order to realize intense excitation and high signal-to-noise ratio on a 2D spectrum, a multiplex Fourier transform technique was adopted. For the excitation, a tandem Fabry-Pérot interferometer (tandem FPI) was used to modulate the excitation light instead of grating-based devices for tuning the wavelength of

excitation light, because the throughput of the interferometer is larger than that of a grating or a prism by approximately one order of magnitude. In addition to the advantage of the multiplex technique using the interferometer, the main advantage of the tandem FPI is applicable to the modulation of transition with a large absorption bandwidth (larger than 100 THz), and is thus applicable to the modulation of the excitation of molecules in the condensed phase.

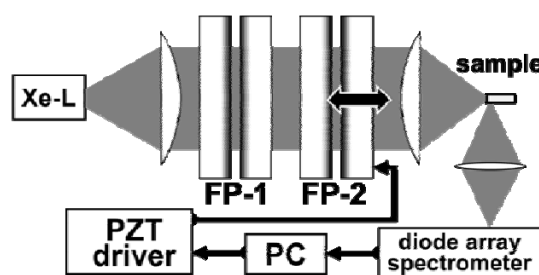


**Figure 1.** Schematic setup of FT-2DFES. FP-1 and FP-2: Fabry-Pérot interferometer, Xe-L: Xe lamp. Mirror gap of FP-2 is controlled by a PZT stage.

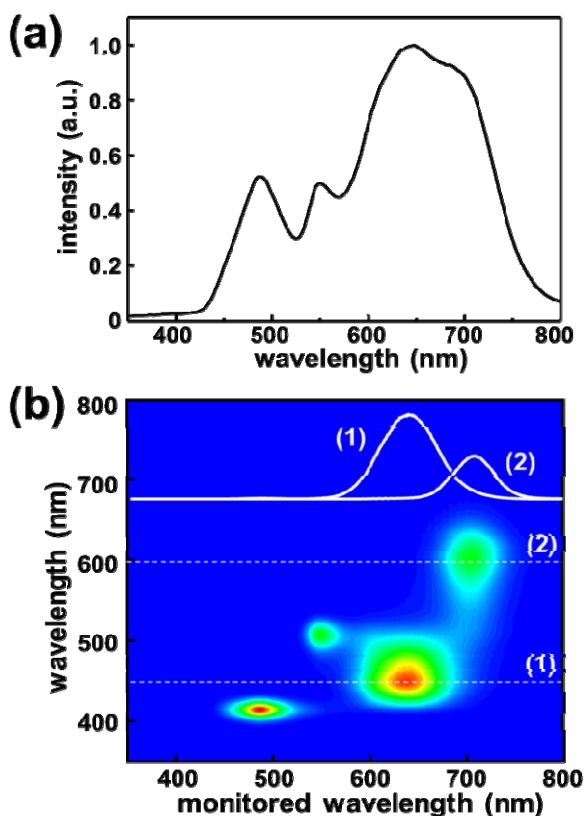


**Figure 2.** (a) Fluorescence spectrum of mixed solution. (b) 2D fluorescence excitation spectrum of mixed solution. Solid curves (1) and (2) are cross sections indicated by dashed lines (1) and (2), respectively.

In order to demonstrate the effectiveness of the FT-2DFES based on the tandem FPI, the 2D-FES was compared with a one-dimensional fluorescence spectrum of the mixed methanol solution of coumarin 480, rhodamine 6G, DCM, and LDS750, as described in Experimental. Figure 2(a) shows a one-dimensional fluorescence spectrum of the mixed methanol solution excited by white light from the Xe lamp. All of the observed peaks overlapped with each other. Figure 2(b) shows the 2D-FES of the mixed methanol solution and the cross sections at the excitation frequencies indicated by dashed lines

(1) and (2). The spectra are represented by solid lines (1) and (2), respectively. All the peaks are well separated. In particular, the overlapping peaks around 650 nm in the one-dimensional fluorescence spectrum were separately observed at approximately 630 nm and 700 nm, as shown by solid lines (1) and (2), respectively.

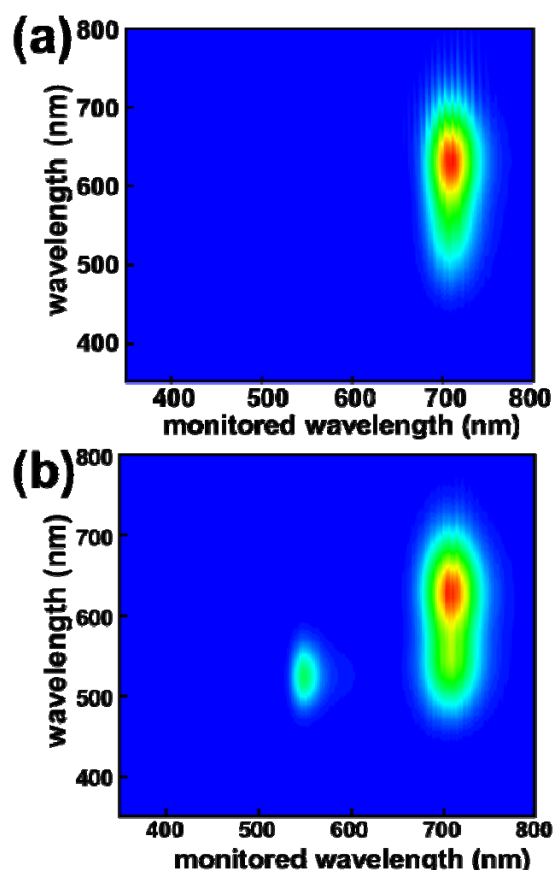


**Figure 3.** 2D fluorescence excitation spectrum of (a) LDS750 and (b) mixed solution of Rhodamine 6G and LDS750.

Figure 3 shows the 2D-FES of (a) LDS750 and (b) a mixed solution of rhodamine 6G and LDS750. By comparing Figure 6(a) with Figure 6(b), it is clear that the 2D peak profile of LDS750 observed at approximately 700 nm is different between the two figures in the high

excitation frequency region. The results suggest that the difference would be caused by the energy transfer from rhodamine 6G to LDS750, because it is well known that energy transfer occurs from

rhodamine 6G to malachite green, whose absorption peak overlaps with the fluorescence peak of rhodamine 6G.

### I-C. HIGH-RESOLUTION SPECTROSCOPY OF POLIATOMIC MOLECULES

Doppler-free high-resolution spectroscopic techniques are powerful tools for studying the structure and dynamics of excited polyatomic molecules in detail and unambiguously. Single-mode auto-scan laser systems in UV-Visible region, the absolute wavenumber measurement system, and several Doppler-free high-resolution spectroscopic measurement systems have been constructed to investigate the excited molecules. High-resolution and high-accuracy of the spectral lines enable to observe rotational-resolved electronic transition and to find out the excited state dynamics through the fairly deviation of the spectral line position, intensity anomaly and the change of the spectral linewidth. Recently, we observed the high-resolution spectrum and Zeeman effect of the  $\pi$ - $\pi^*$  transition of several aromatic molecules such as benzene, naphthalene, anthracene, etc. From the rotational-resolved high-resolution spectrum, the molecular constants were determined in high-accuracy. For all these molecules, the Zeeman broadenings were also observed. The observed Zeeman splittings of the above several aromatic molecules were very small, and it was mainly observed for the levels of low  $K_a$ . The magnitude of Zeeman splitting was increasing in proportion to  $J$  for given  $K_a$ . These results indicate the magnetic moment is along to  $c$ -axis (out of plane) and originates from an electronic angular momentum induced by  $J$ - $L$  coupling between the  $S_1$  and  $S_2$  states. It is concluded that the magnetic moment comes from the orbital angular momentum of electrons and the main nonradiative process in the  $S_1$  state of the isolated benzene, naphthalene, and anthracene molecules is not the intersystem crossing to the triplet state, but the internal conversion to the ground state. We also observed the high-resolution spectrum of 2-Cl naphthalene and 1-Cl naphthalene, which are expected spin-orbit interaction from the heavy-atom effect.

#### High-resolution UV Laser Spectroscopy of $S_1 \leftarrow S_0$ Transition of chloronaphthalene

Ryo Yamamoto, Kenichirou Kanzawa, Takumi Nakano, and Shunji Kasahara

(30th Symposium on Chemical Kinetics and Dynamics)

High-resolution Laser spectroscopy is a useful method to investigate the excited state dynamics such as ISC (Intersystem crossing), IC (Internal conversion), and IVR (Intramolecular vibrational-energy redistribution) is caused by interaction among states. For many polyatomic molecules,  $S_1 - S_0$  transition is expected to be observed in the UV region. We measured high-resolution fluorescence excitation spectrum

of the 0-0 band of the  $S_1 - S_0$  transition of 1- and, 2-Cl naphthalene around 320 nm. In the case of 2-Cl naphthalene, high-resolution fluorescence excitation spectrum had been reported [2]. In this study, we have also observed the rotationally-resolved high-resolution spectrum of 2-Cl naphthalene and its Zeeman effect. Additionally, we observed high-resolution fluorescence excitation spectrum of the 0-0 band of the  $S_1 - S_0$  transition of 1-Cl naphthalene.

A collimated molecular beam of Cl naphthalene was obtained with a pulsed nozzle and a skimmer set up in the vacuum chamber. Sub-Doppler fluorescence excitation spectra were measured by crossing a single-mode UV Laser

beam perpendicular to a collimated molecular beam. Absolute wavenumber was calibrated with accuracy  $0.0002\text{ cm}^{-1}$  by measuring Doppler free saturation spectrum of iodine and fringe pattern of the stabilized etalon.

Rotational structure of 1-Cl naphthalene was observed, but each rotational line was not fully resolved because of the lifetime broadening [3]. Then we determined the molecular constants of 1-Cl naphthalene from the comparison the observed spectrum with calculated one. The Zeeman broadening was not found up to 1.2T. It is suggested that ISC at 0-0 band of the  $S_1 - S_0$  transition 1-Cl naphthalene may be small. Recently,



1-Cl naphthalene



2-Cl naphthalene

### High-resolution Laser Spectroscopy of Vibronic Bands of the Naphthalene $S_1 \leftarrow S_0$ Transition

Takumi Nakano, Ryo Yamamoto, and Shunji Kasahara

(30th Symposium on Chemical Kinetics and Dynamics)

Naphthalene is a simple polycyclic aromatic molecule, and it is interesting that the excited state dynamics such as internal conversion (IC), intramolecular vibrational energy redistribution (IVR), and intersystem crossing (ISC) take place. Thus, a lot of studies for these excited state dynamics have been carried out by many groups. [1,2] In particular, it is reported that non radiative transition to other vibrational levels in the same

we also measured high-resolution fluorescence excitation spectrum of a vibronic band, which lies  $476\text{ cm}^{-1}$  above the 0-0 band of  $S_1 - S_0$  transition, of 2-Cl naphthalene and rotationally-resolved spectrum was obtained. We are trying to analyze it and measure the other vibronic bands.

### References

- [1] H. Katô, M. Baba, and S. Kasahara, *Bull. Chem. Soc. Jpn.* **80**, 456 (2007)
- [2] D. F. Plusquellic, S. R. Davis, and F. Jahanmir, *J. Chem. Phys.* **115**, 225 (2001)
- [3] B. A. Jacobson, J. A. Guest, F. A. Novak, and S. A. Rice, *J. Chem. Phys.* **87**, 269 (1987)

excited state (IVR) efficiently proceeds in the vibronic bands whose vibrational energy exceed  $2122\text{ cm}^{-1}$  from 0-0 band of  $S_1-S_0$  transition (exceed  $0^0_0 + 2122\text{ cm}^{-1}$  band). [1] We have reported about several vibronic bands. [3] In this work, we have measured high-resolution fluorescence excitation spectra of the  $0^0_0 + 2866\text{ cm}^{-1}$  and  $0^0_0 + 3068\text{ cm}^{-1}$  bands of the  $S_1-S_0$  transition of naphthalene.

A jet-cooled molecular beam is obtained by expanding of Ar gas seeded in heated naphthalene vapor in the vacuum chamber. This beam was collimated by a skimmer and a slit. High-resolution fluorescence excitation spectra were observed by crossing of single-mode UV

laser and collimated molecular beam perpendicularly. Absolute wavenumber was calibrated by simultaneously measurement of Doppler-free absorption spectrum of I<sub>2</sub> molecule and transmitting light intensity of the I<sub>2</sub> stabilized etalon.

Observed spectrum of the 0<sup>0</sup><sub>0</sub> + 2866 cm<sup>-1</sup> band is shown in Figure 1. Rotational lines were almost resolved. The background signal of 0<sup>0</sup><sub>0</sub> + 2866 cm<sup>-1</sup> band is larger than the one of lower vibronic bands. On the other hand, rotational lines were not completely resolved for the 0<sup>0</sup><sub>0</sub> + 3068 cm<sup>-1</sup> band, and the background signal of this band was almost twice compared to the one of 0<sup>0</sup><sub>0</sub> + 2866 cm<sup>-1</sup> band. These facts indicate that IVR

process more efficiently proceeds because these vibronic band have high vibrational energy. We estimated the molecular constants of 0<sup>0</sup><sub>0</sub> + 2866 cm<sup>-1</sup> and 0<sup>0</sup><sub>0</sub> + 3068 cm<sup>-1</sup> bands by the comparison between observed and calculated spectra.

#### References

- [1] S. M. Beck, J. B. Hopkins, D. E. Powers, and R. E. Smalley, *J. Chem. Phys.* **74**, 43 (1981)
- [2] F. M. Behlen, and S. A. Rice, *J. Chem. Phys.* **75**, 5672 (1981)
- [3] K. Yoshida, Y. Semba, S. Kasahara, T. Yamanaka, and M. Baba, *J. Chem. Phys.* **130**, 19304 (2009)

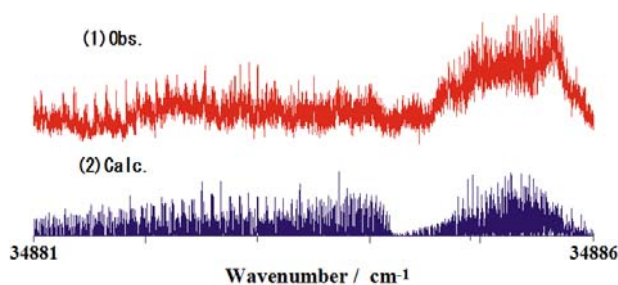


**Figure 1.** Fluorescence excitation spectrum of (1) 0<sup>0</sup><sub>0</sub> + 2866 cm<sup>-1</sup> band of the S<sub>1</sub>-S<sub>0</sub> transition of naphthalene and (2) the calculated spectrum

#### I-D. HIGH-RESOLUTION SPECTROSCOPY OF NO<sub>3</sub> RADICAL

Doppler-free high-resolution spectroscopy was applied to investigate the electronic states of radicals. The radicals are very sensitive to the magnetic field because the spin quantum number is a half integer, it is expected to observe large Zeeman splitting even in the small magnetic field. The Zeeman splitting is very useful to assign the observed rotational lines even in the strong perturbing region. The nitrate radical NO<sub>3</sub> has been known as an important intermediate in chemical reaction in the night-time atmosphere. NO<sub>3</sub> radical belongs with D<sub>3h</sub> point group at the ground state X<sup>2</sup>A<sub>2</sub>'. The three lowest electronic states X<sup>2</sup>A<sub>2</sub>', A<sup>2</sup>E'', and B<sup>2</sup>E' are coupled by vibronic interaction, and therefore NO<sub>3</sub> radical becomes one of the model molecule for understanding the Jahn-Teller (JT) and pseudo Jahn-Teller (PJT) effects. The A-X electronic transition is forbidden, but the weak absorption spectra through the interaction were already observed and reported. On the other hand, the allowed B-X transition has been observed as a strong absorption and LIF excitation spectrum by several groups. The strongest absorption line at 662 nm is called as 0-0 band of B-X

transition which is used to detect the NO<sub>3</sub> radical in the atmosphere, however, the rotational assignment still remained because it is too complicated. By using Doppler-free high-resolution spectroscopic technique, the rotational resolved high-resolution spectrum of the *B-X* 0-0 band was obtained in high-accuracy, and the Zeeman splittings were also measured up to 360 Gauss, and it is very useful to identify the assignment and the coupling unambiguously.

**High-resolution laser spectroscopy and magnetic effect of the  $B^2E' \leftarrow X^2A_2'$  transition of  $^{14}\text{NO}_3$  radical**

**Kohei Tada, Wataru Kashihara, Masaaki Baba<sup>1</sup>, Takashi Ishiwata<sup>2</sup>, Eizi Hirota<sup>3</sup>, and Shunji Kasahara**

<sup>1</sup>Kyoto University, <sup>2</sup>Hiroshima City University,

<sup>3</sup>The Graduate University for Advanced Studies  
(*J. Chem. Phys.* 2014)

Rotationally resolved high-resolution fluorescence excitation spectra of  $^{14}\text{NO}_3$  radical have been observed for the 662 nm band, which is assigned as the 0 – 0 band of the  $\tilde{B}^2E' \leftarrow \tilde{X}^2A_2'$  transition, by crossing a single-mode laser beam perpendicularly to a collimated molecular beam. More than 3000 rotational lines were detected in 15070 – 15145 cm<sup>-1</sup> region, but it is difficult to find the rotational line series. Remarkable rotational line pairs, whose interval is about 0.0246

cm<sup>-1</sup>, were found in the observed spectrum. This interval is the same amount with the spin-rotation splitting of the  $\tilde{X}^2A_2'$  ( $v = 0, k = 0, N = 1$ ) level. From this interval and the observed Zeeman splitting up to 360 G, seven line pairs were assigned as the transitions to the  $^2E'_{3/2}$  ( $J' = 1.5$ ) levels, and fifteen line pairs were assigned as the transitions to the  $^2E'_{1/2}$  ( $J' = 0.5$ ) levels. From the rotational analysis, we recognized that the  $^2E'$  state splits into  $^2E'_{3/2}$  and  $^2E'_{1/2}$  by the spin-orbit interaction, and the effective spin-orbit interaction constant was roughly estimated as -21 cm<sup>-1</sup>. From the number of the rotational line pairs, we concluded that the complicated rotational structure of this 662 nm band of  $^{14}\text{NO}_3$  mainly owes to the vibronic interaction between the  $\tilde{B}^2E'$  state and the dark  $\tilde{A}^2E''$  state through the  $a_2''$  symmetry vibrational mode.

**High-resolution laser spectroscopy and magnetic effect of the  $B^2E' \leftarrow X^2A_2'$  transition of the  $^{15}\text{N}$  substituted nitrate radical**

**Kohei Tada, Kanon Teramoto, Takashi Ishiwata<sup>1</sup>, Eizi Hirota<sup>2</sup>, and Shunji Kasahara**

<sup>1</sup>Hiroshima City University

<sup>2</sup>The Graduate University for Advanced Studies  
(*J. Chem. Phys.* 2015, *in press.*)

Rotationally resolved high-resolution fluorescence

excitation spectra of the 0 – 0 band of the  $\tilde{B}^2E' \leftarrow \tilde{X}^2A_2'$  transition of the  $^{15}\text{N}$  substituted nitrate radical ( $^{15}\text{NO}_3$ ) were observed for the first time, by crossing a jet-cooled molecular beam and a single-mode dye laser beam at right angles. Several thousand rotational lines were detected in the 15080 – 15103 cm<sup>-1</sup> region. We observed the Zeeman splitting of intense lines up to 360 G in order to obtain secure rotational assignment. Two,

nine, and seven rotational line pairs with 0.0248  $\text{cm}^{-1}$  spacing were assigned to the transitions from the  $\tilde{X}^2A_2'$  ( $v'' = 0, k'' = 0, N'' = 1, J'' = 0.5$  and 1.5) to the  ${}^2E'_{3/2}$  ( $J' = 1.5$ ),  ${}^2E'_{1/2}$  ( $J' = 0.5$ ), and  ${}^2E'_{1/2}$  ( $J' = 1.5$ ) levels, respectively, based on the ground state combination differences and the Zeeman splitting patterns. The observed spectrum was complicated due to the vibronic coupling between the bright  $\tilde{B}^2E'$  ( $v = 0$ ) state and surrounding dark vibronic states. Some series of rotational lines other than those from the  $\tilde{X}^2A_2'$  ( $J = 0.5$  and 1.5) levels were also assigned by the

ground state combination differences and the observed Zeeman splitting. The rotational branch structures were identified, and the molecular constants of the  $\tilde{B}^2E'_{1/2}$  ( $v = 0$ ) state were estimated by a deperturbed analysis to be  $T_0 = 15098.20(4) \text{ cm}^{-1}$ ,  $B = 0.4282(7) \text{ cm}^{-1}$ , and  $D_J = 4 \times 10^{-4} \text{ cm}^{-1}$ . In the observed region both the  ${}^2E'_{1/2}$  and  ${}^2E'_{3/2}$  spin-orbit components were identified, and the spin-orbit interaction constant of the  $\tilde{B}^2E'$  ( $v = 0$ ) state was estimated to be  $-12 \text{ cm}^{-1}$  as the lower limit.

## II. Ultrafast Photoscience Laboratory

### II-A. LIQUID DYNAMICS STUDIED BY NONLINEAR INFRARED SPECTROSCOPY

Molecular dynamics in liquids are strongly affected by the nature of intermolecular interactions. It is greatly important to obtain the molecular description on relation between the dynamics and interactions in liquids in order to elucidate the solvent dynamical effect on chemical reactions. Fluctuations of the vibrational transition energies, which are characterized by time correlation functions of the frequency fluctuations, are very sensitive to the dynamics of surrounding environments. Vibrational energy relaxation is also affected by short-range solvent-oscillator interaction. Furthermore, orientational relaxation reflects microscopic viscosity around the oscillator. In recent years, a great deal of effort has been devoted to investigate solute-solvent interactions with infrared (IR) nonlinear spectroscopy. The vibrational frequency fluctuations can be investigated by three-pulse photon echo and two-dimensional IR spectroscopy. By polarization-sensitive pump-probe spectroscopy in the IR region we can study vibrational energy relaxation and orientational relaxation.

#### **Vibrational Dynamics on Non-Ionic Molecules in Aqueous Solution Studied by Two-Dimensional Infrared Spectroscopy**

**Masaki Okuda, Masahiro Higashi,<sup>1</sup> Kaoru Ohta, Shinji Saito,<sup>2</sup> and Keisuke Tominaga**

<sup>1</sup>University of the Ryukyus

<sup>2</sup>Institute for Molecular Science

*(Asian Academic Seminar and School 2015)*

In aqueous solution, water molecules form three-dimensional hydrogen-bonding network, which continuously repeat the rearrangement of its structure. Such a structural fluctuation causes the large energy fluctuation in the systems, and the vibrational and electronic states of a solute molecule are affected by the energy fluctuation. So far, ions are used as probe molecules to study the vibrational dynamics in aqueous solution. In this study, we examine the frequency fluctuation of 2-nitro-5-thiocyanatobenzoic acid (NTBA). Because this molecule has benzene ring, it is expected that we can obtain knowledge of the hydrophobic effects on the frequency fluctuations

by comparing this study and previous studies. The frequency time correlation function (FTCF) was obtained by two-dimensional infrared (2D-IR) experiment. It is found that the FTCF of NTBA in H<sub>2</sub>O can be expressed by a double-exponential function with sub-picosecond and picosecond components. However, the contribution of static component to the FTCF of NTBA is very small. We have reported that the FTCFs of various anion molecules in aqueous solutions also can be expressed by the same function and the slow component of about 1 ps, which is originated from the structural fluctuation of the hydrogen-bond network around solute molecules, does not significantly depend on the solute molecules [1]. In this study, it is shown that the slow component in the FTCF of NTBA in H<sub>2</sub>O can be characterized by the time constant of 1.0 ps. From these results, it can be considered that the dynamics of hydrogen-bond network around NTBA is not significantly different from that around anion molecules.

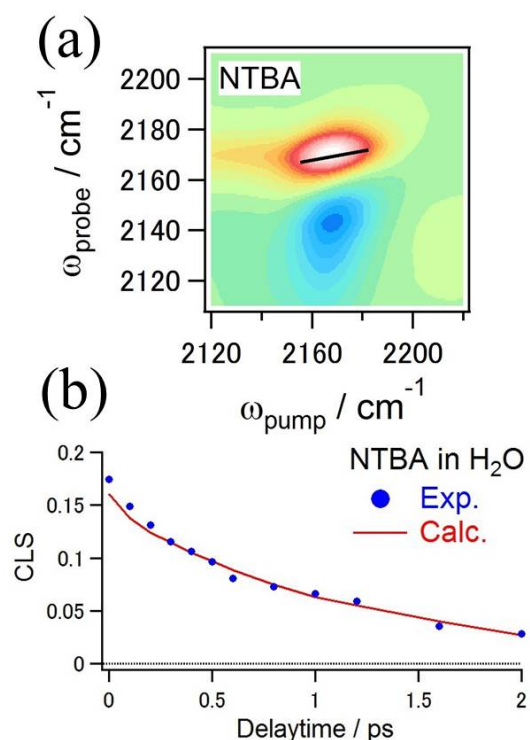


**Figure 1.** (a) The 2D-IR spectra of CN stretching mode of NTBA in H<sub>2</sub>O at population time  $T = 0$  ps. The black line in the spectrum indicates centre line of the spectrum. (b) The CLS curve of NTBA in H<sub>2</sub>O is plotted against population time  $T$ . The curve is proportional to the frequency time-correlation function of the vibrational mode [2]. (Blue) Experimental data, (Red) Calculated data.

- [1] K. Ohta *et al.*, *Acc. Chem. Res.*, **45**, 1982 (2012).  
 [2] K. Kwak *et al.*, *J. Chem. Phys.*, **127**, 124503 (2007).

### Vibrational Dynamics of Nitrosyl Stretch of Ru Complex in Aqueous Solution Studied by Two-Dimensional Infrared Spectroscopy

Kaoru Ohta, Kyoko Aikawa, and Keisuke Tominaga

(*Ultrafast Phenomena 2014*)

To understand the molecular origin of vibrational dynamics in detail, we chose the NO stretching mode of  $[\text{RuCl}_5(\text{NO})]^{2-}$  as a vibrational probe. Here we investigated the temperature dependence of the vibrational frequency fluctuation of the NO stretching mode in aqueous solution and compared with our previous studies of a couple of different ionic probe molecules. Temperature dependence of the vibrational dynamics of the solute in solution provides the systematic information about the coupling between the vibrational mode of the solute and the bath degrees of the system.

To quantify the frequency-frequency correlation functions of vibrational transitions, we used two-dimensional IR spectroscopy. Home-built optical parametric amplifier and difference frequency generators were used to produce a mid-IR pulse at around  $1900 \text{ cm}^{-1}$ . 2D IR spectra were measured with a collinear pulse pair pump-probe geometry. From the FT-IR spectra of the NO stretching mode of  $[\text{RuCl}_5(\text{NO})]^{2-}$ , the peaks of the absorption spectrum are located at around  $1882 \text{ cm}^{-1}$  in D<sub>2</sub>O and H<sub>2</sub>O. We measured the vibrational population relaxation for this mode by ultrafast IR pump-probe spectroscopy. We found that vibrational relaxation takes place on 31 ps in D<sub>2</sub>O and 7.7 ps in H<sub>2</sub>O, respectively. Similar fast relaxations in H<sub>2</sub>O were observed for the other vibrational modes such as anti-symmetric stretching modes of  $\text{N}_3^-$  and  $\text{SCN}^-$  [2]. This is because the vibrational bands at around  $1900 \text{ cm}^{-1}$  couples

strongly with a combination band of the bending and librational modes of H<sub>2</sub>O. Spectral overlap of the solvent vibrational modes enhances the vibrational energy transfer from solute to solvent.

Figure 1 displays 2D-IR spectrum the NO stretching mode of [RuCl<sub>5</sub>(NO)]<sup>2-</sup> in D<sub>2</sub>O taken at 283 K and 313 K. At small values of population times, the 2D IR line shape is elongated along diagonal axis which reflects a positive correlation between the initial ( $\omega_{\text{pump}}$ ) and final ( $\omega_{\text{probe}}$ ) frequencies. At longer population times, the shape becomes more round, reflecting the loss of the correlation of transition frequency. To determine the form of the frequency-frequency correlation function from 2D IR spectra, we used center line slope (CLS) analysis. From the previous studies, the temporal profiles of the CLS mirror the

frequency-frequency correlation function of the vibrational transitions. Figure 1(c) shows the decay profiles of CLS at different temperatures. At 293 K, the decay time constant of CLS is 1.0 ps. This process reflects the hydrogen bonding dynamics under thermal equilibrium condition. The obtained time constant is very similar to that observed in the other ionic vibrational probes [1,2]. This means that time scales of the vibrational frequency fluctuation are not simply determined by the interaction between solute and nearest solvent. Collective dynamics of the solvent molecules around solute play a major role in determining the time scales of the vibrational frequency fluctuations in aqueous solutions.

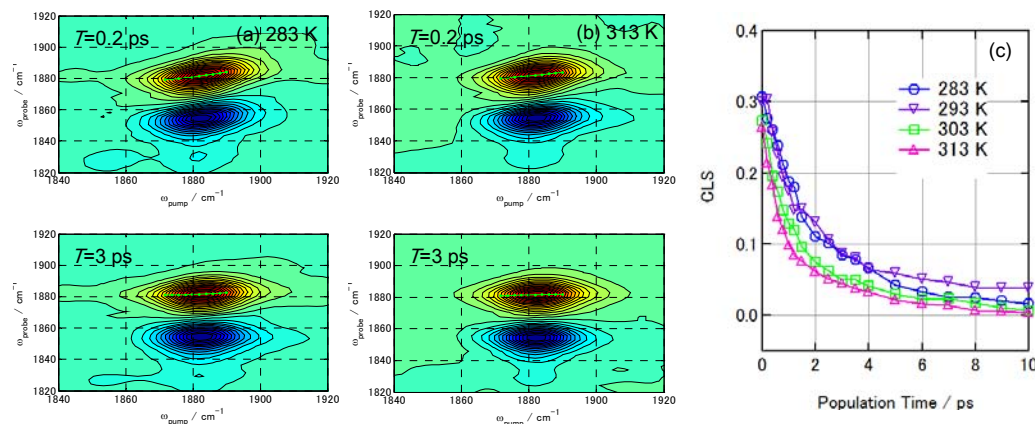


**Figure 1.** (a) 2D IR spectra measured at 283 K with the population times of 0.2 ps and 3 ps. (b) 2D IR spectra measured at 313 K. Green lines and dots are the center line slopes. (c) Temporal profiles of CLS at temperatures of 283 K, 293 K, 303 K and 313 K.

*Chem. Chem. Phys.* **14**, 10455 (2012).

[2] K. Ohta, J. Tayama, S. Saito and K. Tominaga, *Acc. Chem. Res.* **45**, 1982 (2012).

[1] K. Ohta, J. Tayama, and K. Tominaga, *Phys.*

**Solute-solvent interactions of benzonitrile in solutions studied by sub-picosecond infrared pump-probe spectroscopy**

**Motohiro Banno, Ayumi Kotani, Kaoru Ohta, and Keisuke Tominaga**

*(Bull. Chem. Soc. Jpn., 2014)*

The vibrational energy relaxation of the CN stretching mode of benzonitrile (BN) in solution has been investigated by infrared (IR) pump-probe spectroscopy. The peak wavenumber, lineshape, and cross section of the ground state absorption band due to the CN stretching mode depend on the solvent and concentration. From the experimental results of IR spectroscopic methods and calculations with the density functional theory, the structures of solute-solute or solute-solvent complexes are suggested. In hexane, BN exists as the monomer or

the dimer in which the two CN groups are arranged in the anti-parallel way. In ethanol (EtOH), it is suggested that BN forms the anti-parallel dimer and a BN-EtOH hydrogen-bonded complex. In dimethylsulfoxide (DMSO), BN probably forms a solute-solvent complex. From the results of IR pump-probe spectroscopy, the decay time constant of the pump-probe signal shows a probe wavenumber dependence in hexane and DMSO, which indicates inhomogeneity of the microscopic environment around BN in these solvents. In EtOH, the wavenumber dependence was not observed. The result suggests that the VER processes for the BN dimer and the BN-EtOH complex are accelerated from that for the monomer, and the VER times are almost identical among the two structures.

## **II-B. DYNAMICS OF ELECTRONICALLY EXCITED STATE IN CONDENSED PHASES**

Understanding of dynamics in the electronically excited state is a key issue to elucidate mechanisms in various photochemical reactions in condensed phases. It is also important for designing and developing new materials which have characteristic functions. We employ various kinds of ultrafast technique to monitor photochemical and photophysical events in sub-pico- to picoseconds time scales. By femtosecond fluorescence up-conversion technique, dynamics in the electronically excited state can be observed with a time resolution up to 100 fs. Vibrational dynamics in the electronically excited can be investigate by UV/VIS-pump IR probe technique. Moreover, low-frequency responses by photoexcitation are investigated by UV/VIS-pump THz probe experiment. Such responses include change of low-frequency vibrational modes induced by photoexcitation and photo-induced changes of charge carrier dynamics.

**Vibrational Dynamics of the CO Stretching of 9-Fluorenone Studied by Visible-pump and Infrared-probe Spectroscopy**

**Yuki Fukui, Kaoru Ohta, and Keisuke Tominaga**

*(Faraday Discussion)*

In a solution, a solute molecule relaxes to the most stable state of the electronically excited state ( $S_1$ ) after the electronic excitation through various

relaxation processes. These processes are, for example, a vibrational energy relaxation, a cooling process of the locally heated environment around the solute, and solvation dynamics. They influence chemical reactions initiated by the electronic excitation. In a protic solvent, a solute molecule forms intermolecular hydrogen bonds with solvents if the solute has hydrogen bonding sites such as a carbonyl group. The hydrogen bonds influence various properties of solute such as its electronic states, the relaxation processes, and so on. 9-Fluorenone (FL) has a carbonyl group which can form hydrogen bonds. The vibrational dynamics of FL in alcohol solutions are previously reported in the electronically ground state and excited states. In this study, we studied effects of hydrogen bond on the vibrational structures and the vibrational dynamics of the CO stretching mode of the excited state FL in various solvents

### **Vibrational Dynamics of the CN Stretching in the Electronically Excited State by Visible-Pump and Infrared-Probe Spectroscopy**

**Sho Hiraoka, Kaoru Ohta, and Keisuke Tominaga**

*(Ultrafast Phenomena 2014)*

Understanding of mechanisms of photochemical reactions in solution is one of the important problems in current chemistry. After photoexcitation to the electronically excited state of a solute molecule in solution, various relaxation processes occur such as vibrational energy relaxation or solvation dynamics. The fate of the excited state is strongly influenced by these relaxation processes, therefore, it is very important to understand these relaxation processes in detail.

including alcohol by sub-picosecond visible-pump and IR-probe spectroscopy.

We measured the visible-pump and IR-probe signals in various solvents including alcohol. The transient IR spectrum of the CO stretching band in methanol-*d*<sub>4</sub> has peaks at 1530 cm<sup>-1</sup> and 1555 cm<sup>-1</sup>. We assigned the two bands at 1530 cm<sup>-1</sup> and 1555 cm<sup>-1</sup> to a FL complex with solvents and free FL, respectively. In all the solvents, the CO stretching bands show blue-shifts in time. A possible mechanism for this blue-shift is vibrational cooling. Vibrational cooling is derived from anharmonic couplings by some low frequency modes. This cooling process of the locally heated environment around the solute influences the blue-shifts. However, red-shift is observed at later time for the band at 1530 cm<sup>-1</sup> in methanol-*d*<sub>4</sub>. A possible mechanism of this spectral shift is reorganization of solvent which form hydrogen bonds with FL.

On the other hand, hydrogen-bonding liquids such as water and alcohol form characteristic network structures, which affect various properties of a solute molecule such as the electronic state and vibrational structures. In this work, we focus on the vibrational dynamics of a solute in the electronically excited state in alcohol solutions. The vibrational mode we investigate is the CN stretching mode of 3-cyano-7-hydroxy-4-methyl coumarin (C183m, Figure 1). Generally, coumarin dyes change their permanent dipole moments largely by photoexcitation, causing change of the dielectric interaction between the dyes and surrounding solvents. We have carried out visible-pump and infrared (IR)-probe spectroscopic measurements on this mode to examine influence of

the solvent interactions on the vibrational dynamics of the solute.

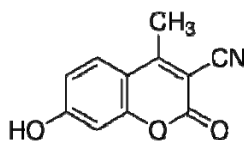


**Figure 1.** Structure of C183m.

The transient IR spectra of the CN stretching band are shown in Figure 2. There are a bleach centered at  $2225\text{ cm}^{-1}$  and a transient absorption at  $2180\text{ cm}^{-1}$ , and we fit the transient spectra with a sum of two Gaussian functions to determine the peak wavenumber of the transient absorption component. The peak of the CN stretching mode shows a blue shift with delay time, and the time-dependence of this blue shift is reproduced well by a single exponential with a time constant of about 10 ps. One of the possible mechanisms for this blue shift is vibrational cooling. Vibrational cooling resulted from anharmonic couplings between the high-frequency mode and some low-frequency modes. Just after the photoexcitation the local temperature around the solute is higher than the room temperature because of the dissipation of the excess energy, causing population in the higher vibrational states of the low-frequency modes. This vibrational cooling has been observed in several transient vibrational spectroscopic studies [1,2]. Another possible mechanism for the blue shift is solvation dynamics. If the photoexcitation accompanies a large change of the dipole moment of the solute, dielectric response from the polar solvent causes the stabilization of the electronic and vibrational states of the solute. Depending on the directions of the permanent dipole moments of the  $S_0$  and  $S_1$  states

and the charge distribution in the normal modes, the peak wavenumber shifts either the blue side or red side during the solvation dynamics. We further carried out UV-pump and IR-probe measurement, where the third harmonics at 266 nm was used as a pump pulse. In this case the excess energy is about  $12450\text{ cm}^{-1}$ , which is much larger than that of the second harmonic excitation ( $1420\text{ cm}^{-1}$ ). The transient absorption spectrum at  $t=0$  ps is further blue-shifted compared to the second harmonic excitation case, and the time-dependence of the blue shift can be described by a similar time constant to that of the vis-pump case. These results suggest that the blue shift is caused by vibrational cooling rather than solvation dynamics, since the total shift due to vibrational cooling depends on the excess energy whereas that due to solvation dynamics does not depend on it so much.

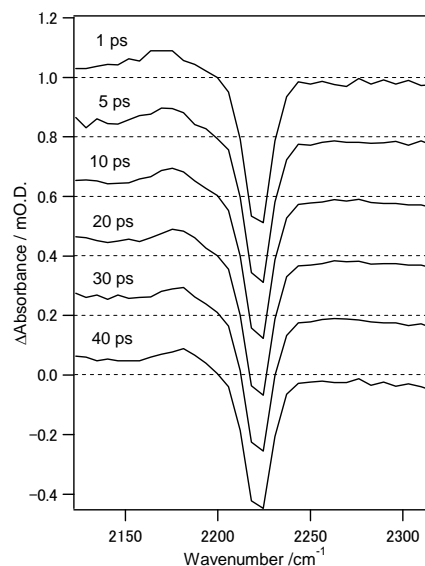


**Figure 2.** Transient absorption spectra of C183m in  $\text{CH}_3\text{OH}$  at different delay times.

[1] P. Hamm, S. M. Ohline, and W. Zinth, *J. Chem. Phys.* **106**, 519 (1997).

[2] K. Iwata and H. Hamaguchi, *J. Phys. Chem. A*, **101**, 632 (1997).

**Time-Resolved Fluorescence Spectroscopy Study of Excited State Dynamics of Alkyl- and Benzo-Substituted Triphyrin(2.1.1)**

**Yusuke Iima, Daiki Kuzuhara,<sup>1</sup> Zhao-Li Xue,<sup>1</sup> Seiji Akimoto, Hiroko Yamada<sup>1</sup> and Keisuke Tominaga**

<sup>1</sup>Nara Institute of Science and Technology  
(*Phys. Chem. Chem. Phys.*, 2014)

We have investigated the photophysical properties of alkyl-substituted triphyrin(2.1.1) (ATp) and benzotriphyrin(2.1.1) (BTp) by steady-state and time-resolved fluorescence spectroscopy. We focused on the effect of NH proton tautomerization, planarity of the macrocycles, and substituents on these properties. The fluorescence quantum yields

( $\Phi_y$ ) of ATp did not depend on solvent viscosity, whereas those of BTp increased with solvent viscosity, reaching a maximum value of 0.17 in paraffin. Interestingly, analyzing  $\Phi_y$  showed that the non-radiative rate constant of BTp decreased sharply as the solvent viscosity increased. These results suggest that the substituted phenyl groups play a crucial role in suppressing molecular distortion, thus leading to decreased non-radiative relaxation in triphyrin(2.1.1). The hydrogen bond formed in the inner cavity potentially contributes to the suppression of the structural distortion, whereas the pyrrole rings in the macrocycle are close, as in porphycene.

**II-C. MOLECULAR DYNAMICS IN THE TERAHERTZ FREQUENCY REGION IN CONDENSED PHASES**

Vibrational spectroscopy has been widely used to investigate structures, interactions and dynamics of molecules and molecular complexes. The low-frequency region below several terahertz (THz; 1 THz = 33.3 cm<sup>-1</sup>) corresponds to intermolecular modes of complexes and intramolecular modes with a weaker potential force and/or larger reduced mass. Intermolecular interactions such as hydrogen bonding, van der Waals forces and charge-transfer interactions play important roles in various chemical and biological processes. Moreover, the low-frequency spectra also reflect molecular dynamics on a time scale from picoseconds to femtoseconds. There has been dramatic progress in the generation and detection techniques of freely propagating THz radiation in the past two decades. The examples of the generation technique include photoconductive switching, optical rectification, and the surface photocurrent of semiconductors. Because the pulse duration of the THz radiation is in a sub-picosecond time region, it is possible to measure the electric field of the radiation by coherent detection methods, which consequently allows us to conduct THz time-domain spectroscopy (TDS). By THz-TDS we can obtain the refractive index and extinction coefficient of a medium by measuring the phase and amplitude of the radiation. THz-TDS is an attractive method for studying dynamics in condensed phases with time scales of sub-picoseconds and picoseconds. We have applied

THz-TDS to investigate various kinds of condensed materials, including neat liquids and mixtures of liquids, biological polymers, and charge carrier dynamics in semiconductors and conducting polymers.

**Low-frequency dynamics of trehalose-coated lysozyme studied by terahertz time-domain spectroscopy**

**Risa Okada, Naoki Yamamoto<sup>1</sup>, Atsuo Tamura<sup>1</sup>, Keisuke Tominaga**

<sup>1</sup>Kobe University

(ASUD 2014)

Under the extreme conditions such as highly dried state or very low temperature biopolymers like proteins usually denature, leading to damage on organisms. However, some organisms can survive under such extreme conditions without suffering any damage. To protect themselves, these organisms in the dehydrated state contain large amount of sugar, particularly trehalose. Since viscosity of trehalose is very high, it prevents structural changes of biopolymers. When protein changes its structure, large-amplitude motions in the low-frequency region are often activated. Such motions have collective nature and correspond to low-frequency motions below a hundred wavenumbers. In this study, we measured the low-frequency spectra of proteins coated with trehalose from 83 K to 353 K by terahertz time-domain spectroscopy (THz-TDS) to study thermal activation of the low-frequency dynamics affected by sugar coating.

In THz-TDS system, a pair of photoconductive antenna was used for generation and detection of THz electro-magnetic wave. The

sample is trehalose, lysozyme, and trehalose-coated lysozyme. Other disaccharides except trehalose (maltose and sucrose) were also measured. Each of these lyophilized samples in a cell was pressed at a pressure of 8 Mpa to make pellet samples.

Trehalose is crystallized by heating. The absorption coefficient spectra of trehalose are different from trehalose-coated lysozyme when heated. THz absorption coefficients increase linearly with temperature. At around 300 K, the slope of the absorption coefficient of trehalose-coated lysozyme becomes larger. This temperature dependence of trehalose-coated lysozyme by THz-TDS matches with the calorimetric glass transition. We measured complex dielectric constant from GHz to THz by network analyzer (0.2 ~20 GHz) and THz-TDS (0.3 ~2 THz) in order to reveal the motions around glass transition. And we reproduced dielectric spectra in the sum of Cole-Cole relaxation modes and underdamped vibrational modes. In the result, THz dielectric spectra include not relaxation modes but underdamped vibrational modes. So THz dielectric spectra of each temperature are reproduced by two underdamped vibrational modes. We discuss relation between temperature dependence of low frequency dynamics and each of motion.

## **The Low-Frequency Vibration Study of Amino Acids Using Terahertz Spectroscopy and Solid-state Density Functional Theory**

**Feng Zhang, Keisuke Tominaga, Michitoshi Hayashi<sup>1</sup>, and Houg-Wei Wang<sup>1</sup>**

<sup>1</sup>National Taiwan University

(*SPIE Photonics Asia*)

Understanding the low-frequency normal modes of amino acids, the building blocks of proteins, is crucial to reveal the vibration-function relationship in the macromolecular system. Recent advances in terahertz spectroscopy and solid-state density functional theory have ensured the accurate access to low-frequency modes of amino acids. A new knowledge people have learnt so far is that the inter- and intra-molecular vibrations are strongly coupled with each other in the low-frequency (or THz) region through the vibrational coordinate mixing. Rich information is believed embedded in this phenomenon [1,2].

We will introduce an analytical mode-decoupling method that allows for the accurate decomposition of a normal mode of interest into the three intermolecular translations, three principal librations and various intrinsic intramolecular

vibrations. We will demonstrate a theoretical analysis by using the L-alanine system as an example. The mode-decoupling method helps reveal new intramolecular vibrational modes on the first hand, and more importantly, shed light on a new phenomenon of the intramolecular vibrational coordinate distribution (IVCD). IVCD describes the broad distributions of important intramolecular normal modes such as  $\text{NH}_3^+$  torsion,  $\text{COO}^-$  torsion and  $\text{CH}_3$  torsion.

The IVCD concept may imply solutions to a string of unsettled problems relevant to the low-frequency molecular vibrations, e.g. the formation mechanism of the peptide bonds, the explanation of the line shape of  $\text{CH}_3$  tunneling in the small molecular system as well as the first onset of anharmonicity of  $\text{CH}_3$  rotation in the protein system.

1. F. Zhang, O. Kambara, K. Tominaga, J. Nishizawa, T. Sasaki, H.-W. Wang, and M. Hayashi, *RSC Adv.*, **4**, 269-278, (2014).

2. F. Zhang, M. Hayashi, H.-W. Wang, K. Tominaga, O. Kambara, J. Nishizawa, and T. Sasaki, *J. Chem. Phys.* **140**, 174509 (2014).

## **Terahertz spectroscopy and solid-state density functional theory calculation of anthracene: effect of dispersion force on the vibrational modes**

**Feng Zhang, Michitoshi Hayashi<sup>1</sup>, Houg-Wei Wang<sup>1</sup>, Keisuke Tominaga, Ohki Kambara<sup>2</sup>, Jun-ichi Nishizawa<sup>3</sup>, and Tetsuo Sasaki<sup>2</sup>**

<sup>1</sup>National Taiwan University

<sup>2</sup>Shizuoka University

<sup>3</sup>Tohoku University

(*J. Chem. Phys.*, 2014)

The phonon modes of molecular crystals in the terahertz frequency region often feature delicately coupled inter- and intra-molecular vibrations. Recent advances in density functional theory such as DFT-D\* have enabled accurate frequency calculation. However, the nature of normal modes has not been quantitatively discussed against experimental criteria such as isotope shift (IS) and correlation field splitting (CFS). Here, we report an analytical mode-decoupling method that allows for the

decomposition of a normal mode of interest into intermolecular translation, libration, and intramolecular vibrational motions. We show an application of this method using the crystalline anthracene system as an example. The relationship between the experimentally obtained IS and the IS obtained by PBE-D\* simulation indicates that two distinctive regions exist. Region I is associated with a pure intermolecular translation, whereas region II features coupled intramolecular vibrations that are

further coupled by a weak intermolecular translation. We find that the PBE-D\* data show excellent agreement with the experimental data in terms of IS and CFS in region II; however, PBE-D\* produces significant deviations in IS in region I where strong coupling between inter- and intra-molecular vibrations contributes to normal modes. The result of this analysis is expected to facilitate future improvement of DFT-D\*.

### **Intramolecular Vibrations in Low-Frequency Normal Modes of Amino Acids: L-Alanine in Neat Solid State**

**Feng Zhang, Houg-Wei Wang<sup>1</sup>, Keisuke Tominaga, and Michitoshi Hayashi<sup>1</sup>**

<sup>1</sup>National Taiwan University

(*J. Phys. Chem. A*, in press)

This paper presents a theoretical analysis of the low-frequency phonons of L-alanine by using the solid-state density functional theory at the gamma point. We are particularly interested in the intramolecular vibrations accessing low-frequency phonons via vibration mixing with intermolecular

vibrations. A new mode-analysis method is introduced to quantify the vibrational characteristics of such intramolecular vibrations. We find that the torsional motions of COO<sup>-</sup> are involved in low-frequency phonons, although COO<sup>-</sup> is conventionally assumed to undergo localized torsion. We also find the broad distributions of intramolecular vibrations relevant to important functional groups of amino acids, e.g., the COO<sup>-</sup> and NH<sub>3</sub><sup>+</sup> torsions, in the low-frequency phonons. The latter finding is illustrated by the concept of frequency distribution of vibrations. These findings may lead to immediate implications in other amino acid systems.

### **Conduction in Polyaniline Emeraldine Salt in the Terahertz Region: A Temperature Dependence Study**

**Alvin Karlo G. Tapia and Keisuke Tominaga**

(*Chem. Phys. Lett.*, 2014)

The temperature-dependent conductivity of polyaniline emeraldine salt (PAni-ES) was studied by terahertz (THz) time-domain spectroscopy from 80 to 290 K to investigate conduction properties in the THz region. The absorption coefficient and index of

refraction increase with temperature. This reflects an increasing conductivity, which indicates a thermally assisted hopping transition. The frequency-dependent behavior of the conductivity is described by using the Mott-Davis model. The model fitting parameter,  $S$ , decreases with increasing temperature, indicating a possible correlated barrier hopping mechanism. Lastly, the activation energy at THz frequencies decreases with increasing frequency, suggesting intraband transitions.

## Temperature and Hydration Dependence of Complex Dielectric Spectra of Lysozyme from GHz to THz Frequency Region

Naoki Yamamoto, Atsuo Tamura<sup>1</sup>, and Keisuke Tominaga

<sup>1</sup>Kobe University

(8th International Conference on Broadband Dielectric Spectroscopy and its Applications)

Understanding of structures and dynamics of proteins is a fundamental problem for studies on protein function. When protein expresses the function, large structural changes often occur. These changes are induced by the collective motions of many atoms in protein, corresponding to the low-frequency motion below a few tens of wavenumbers. Therefore, the low-frequency spectra of protein contain information on the motions relevant to the function of protein. In this study we obtained and analyzed complex dielectric spectra in the THz region. We studied temperature and hydration dependence on the dielectric spectra of lysozyme from GHz to terahertz (THz) frequency regions.

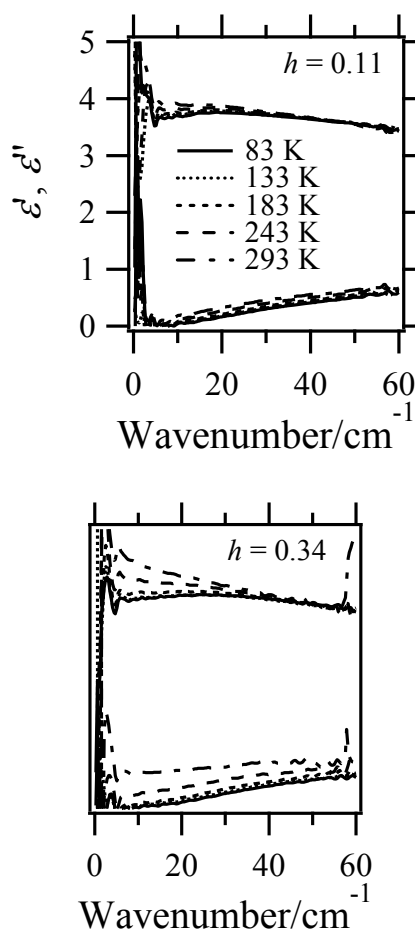


**Figure 1.** Temperature dependence of complex dielectric spectra of the dehydrated state (left) and a hydrated state (right), respectively. In each panel the upper and the lower groups correspond to the real parts and the imaginary parts, respectively. The hydration degree, which is defined by the value of  $h$  (weight of water divided by weight of protein) is shown in each figure.

In both dehydrated and hydrated states the complex dielectric spectra linearly increase as temperature rise below 180 K as shown in Figure 1. However, at higher temperatures the spectral components of the dielectric spectra increase more in the hydrated state than the dehydrated state. We performed spectral analysis of the complex dielectric spectra,  $\epsilon^*(\nu)$ , using some model functions such as a sum of an

underdamped mode and a Cole-Cole function. We discuss temperature dependencies of these parameters obtained from the analysis.

**Temperature and Hydration Dependence of Low-Frequency Spectra of Lipid Bilayers Studied by Terahertz Time-Domain Spectroscopy**

**Naoki Yamamoto, Tomoyo Andachi, Atsuo Tamura<sup>1</sup>, and Keisuke Tominaga**

<sup>1</sup>Kobe University

(*J. Phys. Chem. B*, in press)

We have studied temperature and hydration dependent low-frequency spectra of lipid bilayers of 1,2-dimyristoyl-sn-glycero-3-phosphoryl-3'-rac-glycerol (DMPG) and 1,2-dimyristoyl-sn-glycero-3-phosphocholine (DMPC) by terahertz time-domain spectroscopy (THz-TDS). We measured X-ray diffraction patterns and mid-infrared spectra of these lipid bilayers and found that the lipid bilayer have two different types of phases, i.e. the gel phase and the crystalline phase, depending on preparation methods of the samples. In both the phases a few distinct bands were observed in the THz region. For

DMPG the peak wavenumbers of the absorption bands did not change upon hydration, while the bandwidth in the crystalline phase was smaller than that in the gel phase. We performed spectral analyses for the complex dielectric spectra for DMPG and DMPC with a model function, mainly to determine the peak wavenumbers of the absorption bands. In contrast to the case of the DMPG bilayers the peak wavenumber of the absorption band of the DMPC bilayer shifts upon hydration. In the hydrated DMPC bilayer it was suggested fast reorienting water molecules exist with a relaxation time of sub-picoseconds. It is suggested that the THz absorption patterns reflect the lipid packing pattern in the bilayers. The temperature dependence of the absorption band was analyzed by an empirical equation, and the anharmonicity of the vibrational potential of the low-frequency mode was quantitatively evaluated.

## II-D. EXCITATION RELAXATION DYNAMICS OF PHOTOSYNTHETIC SYSTEMS STUDIED BY TIME-RESOLVED FLUORESENCE SPECTROSCOPY

In photosynthetic systems, solar energy is captured by antenna pigments, such as chlorophylls, carotenoids and phycobiliproteins, which is followed by the energy transfer among photosynthetic pigments and the electron transfer in the reaction centers. It is, therefore, of great importance for the clear understanding of primary processes in photosynthetic reactions to detect signals that reflect ultrafast excited state dynamics after an excitation of pigments. By using short pulses from a Ti:Sapphire laser as light sources for measurements of time-resolved fluorescence spectra in femtosecond to nanosecond region, ultrafast processes in photosynthetic systems are examined.

### Excitation relaxation dynamics and energy transfer in fucoxanthin-chlorophyll *a/c*-protein complexes, probed by time-resolved fluorescence

S. Akimoto, A. Teshigahara<sup>1</sup>, M. Yokono, M. Mimuro<sup>2</sup>, R. Nagao<sup>3</sup>, T. Tomo<sup>4</sup>,

<sup>1</sup>Kobe University, Graduate School of Science, <sup>2</sup>Graduate School of Human and Environmental Studies, Kyoto University, <sup>3</sup>Division of Material Science, Graduate School of Science, Nagoya University, <sup>4</sup>Faculty of Science, Tokyo University of Science

(*Biochim. Biophys. Acta*, 2014)

In algae, light-harvesting complexes contain specific chlorophylls (Chls) and keto-carotenoids; Chl *a*, Chl *c*, and fucoxanthin (Fx) in diatoms and brown algae; Chl *a*, Chl *c*, and peridinin in photosynthetic dinoflagellates; and Chl *a*, Chl *b*, and siphonaxanthin in green algae. The Fx–Chl *a/c*-protein (FCP) complex from the diatom *Chaetoceros gracilis* contains Chl *c*<sub>1</sub>, Chl *c*<sub>2</sub>, and the keto-carotenoid, Fx, as antenna pigments, in addition to Chl *a*. In the present study, we investigated energy transfer in the FCP complex associated with photosystem II (FCPII) of *C. gracilis*. For these investigations, we analyzed

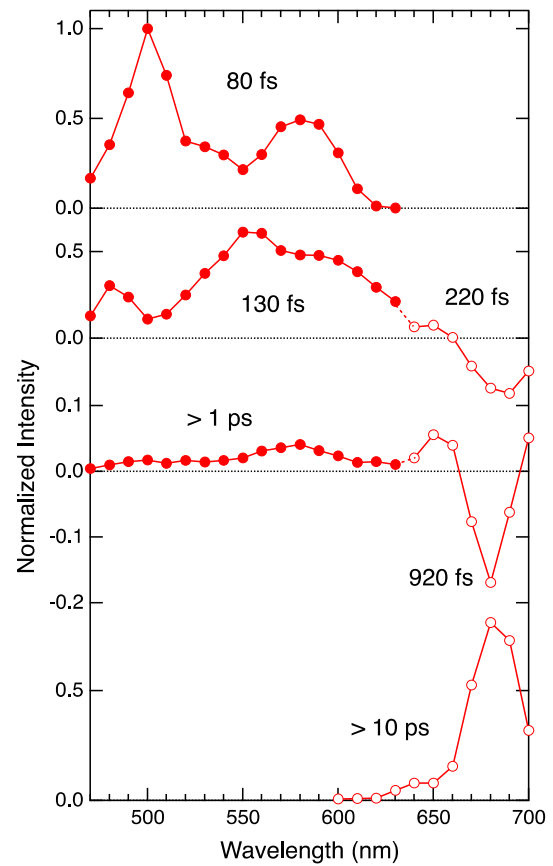


**Figure 1.** Fluorescence decay-associated spectra of FCPII complex excited at 425 nm. Time constants required for analysis in the shorter wavelength region (closed circle) differed from those used for analyses in the longer wavelength region (open circle).

time-resolved fluorescence spectra, fluorescence rise and decay curves, and time-resolved fluorescence anisotropy data. Chl *a* exhibited different energy forms with fluorescence peaks ranging from 677 nm to 688 nm. Fx transferred excitation energy to lower-energy Chl *a* with a time constant of 300 fs. Chl *c* transferred excitation energy to Chl *a* with time constants of 500–600 fs

(intra-complex transfer), 600–700 fs (intra-complex transfer), and 4–6 ps (inter-complex transfer). The latter process made a greater contribution to total Chl *c*-to-Chl *a* transfer in intact cells of *C. gracilis* than in the isolated FCPII complexes. The lower-energy Chl *a* received excitation energy from Fx and transferred the energy to higher-energy Chl *a*.

### Energy transfer processes in chlorophyll *f*-containing cyanobacteria using time-resolved fluorescence spectroscopy on intact cells

T. Tomo<sup>1</sup>, T. Shinoda<sup>1</sup>, M. Chen<sup>2</sup>, S. I. Allakhverdiev<sup>3,4</sup>, S. Akimoto

<sup>1</sup> Faculty of Science, Tokyo University of Science, <sup>2</sup>School of Biological Sciences, University of Sydney, <sup>3</sup>Institute of Plant Physiology, Russian Academy of Science, <sup>4</sup>Institute of Basic Biological Problems, Russian Academy of Sciences  
(*Biochim. Biophys. Acta*, 2014)

We examined energy transfer dynamics in the unique chlorophyll (Chl) *f*-containing cyanobacterium *Halomicronema hongdechloris*. The absorption band of Chl *f* appeared during cultivation of this organism under far-red light. The absorption maximum of Chl *f* in organic solvents occurs at a wavelength of approximately 40 nm longer than that of Chl *a*. In vivo, the cells display a new absorption band at approximately 730 nm at 298 K, which is at a significantly longer wavelength than that of Chl *a*. We primarily assigned this band to a long wavelength form of Chl *a*. The function of Chl *f* is currently unknown. We measured the fluorescence of cells using time-resolved fluorescence spectroscopy in the picosecond-to-nanosecond time range and found

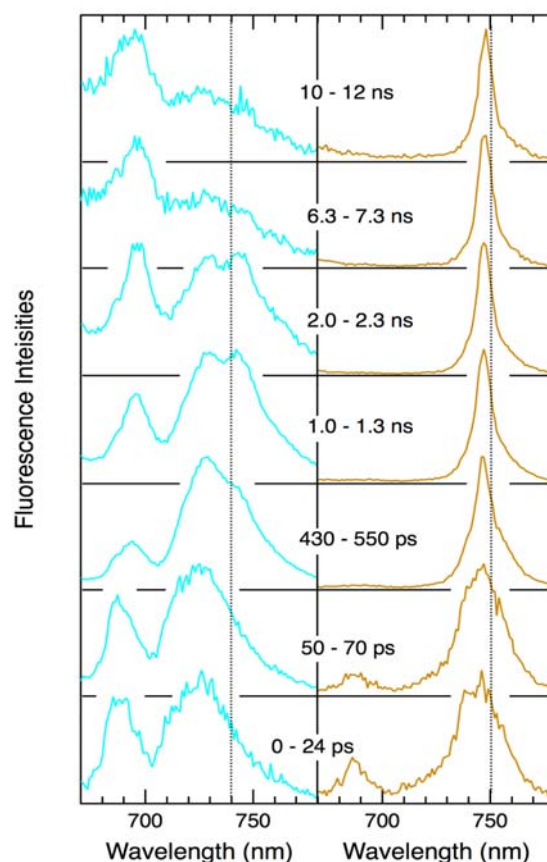


**Figure 1.** Time resolved fluorescence spectra (TRFS) of *H. hongdechloris* cells. Left side: normalized TRFS of the cells cultured under white light. Right hand: normalized TRFS of the cells under far-red light.

clear differences in fluorescence properties between the cells that contained Chl *f* and the cells that did not. After excitation, the fluorescence peaks of photosystem I and photosystem II

appeared quickly but diminished immediately. A unique fluorescence peak located at 748 nm subsequently appeared in cells containing Chl *f*.

This finding strongly suggests that in this alga, Chl *f* exists in both photosystems and that Chl *f* is located close to Chl *a*.

### III Coherent Photoscience Laboratory

#### III-A. HIGH FIELD ELECTRON SPIN RESONANCE (ESR) STUDIES OF QUANTUM SPIN SYSTEMS

Quantum spin system is a magnetic system which shows distinct quantum effects due to its strong quantum fluctuation. Recently, quasi-one dimensional quantum spin systems have attracted much interest, and their short range order and their ground state at low temperature should be clarified. High frequency high field ESR turns out to be a powerful means to observe the short-range order and the ground state of the system. Moreover, frustrated magnetic systems have also attracted much interest recently. The frustration in the magnetic system suppresses the conventional magnetic order and a unique ground state appears at low temperature. Especially the competition is expected between the frustration and low dimensionality. Following the trends from a Grant-in-Aid for Scientific Research on Priority Areas “Novel states of matter induced by frustration” (No.473, 2007-2011, Headed by Prof. H. Kawamura (Osaka University) and H. Ohta was a member), we are studying these low dimensional antiferromagnets with frustration and related multiferroic materials intensively. High Field ESR of multiferroic material  $\text{YCrO}_3$  has been performed and non-conventional AFMR modes, which cannot be interpreted by the molecular field theory, were observed. The master course student S. Ikeda, who presented the ESR study of  $\text{YCrO}_3$ , received the Excellent Presentation Award at Young Frontier Meeting organized by the Center for Supports to Research and Education Activities, Kobe University, and the Best Presentation Award for the Physics Master Course Presentation at Kobe University. H. Ohta gave an invited presentations at International Conference “Magnetic Resonance: fundamental research and pioneering applications (MR-70)” (June 23-27, 2014, Kazan, Russia), “International Symposium Catalytic Systems for Chemical Energy Conversion” (July 23-25, 2014, Mülheim an der Ruhr, Germany), and CONIAPS XVII (January 16-18, 2015, Jaipur, India), and introduced the recent results of high field ESR in Kobe. Especially H. Ohta received the Fellowship Award for his contribution to the developments of high field THz ESR from the International Academy of Physical Sciences during CONIAPS XVII. H. Ohta (Chair), S. Okubo (Secretary), E. Ohmichi, T. Sakurai, S. Hara have organized the joint symposium APES-IES-SEST2014 (Nov. 12-16, 2014, Nara, Japan). The symposium was rather successful with 279 participants from 22 countries which turned out to be a record for APES symposium. In meantime H. Ohta served as the Vice-President of IES (International EPR(ESR) Society) and was appointed as the President of IES since January, 2015. H. Ohta is also acting as the Vice-President of APES (Asia-Pacific EPR/ESR Society), the Secretary General of the Japan Society of Infrared Science and Technology, and the Council Member of SEST. Moreover, in order to strengthen the pulsed magnetic field researches in western Japan region, we have set up The KOFUC (Kobe-Osaka-Fukui Universities Centers) Network, which is intended to strengthen the pulsed magnetic field researches in western Japan region, was approved by the High Magnetic Field Forum of Japan in December, 2014.

**Disappearance of Ising nature in  $\text{Ca}_3\text{ZnMnO}_6$  studied by high-field ESRM**

**Y Ruan<sup>1,2</sup>, Z W Ouyang<sup>1</sup>, Y M Guo<sup>1,2</sup>, J J Cheng<sup>1,2</sup>, Y C Sun<sup>1,2</sup>, Z C Xia<sup>1</sup>, G H Rao<sup>3</sup>, S Okubo<sup>4</sup> and H Ohta<sup>4</sup>**

<sup>1</sup>Wuhan National High Magnetic Field Center, Huazhong University of Science and Technology

<sup>2</sup>School of Physics, Huazhong University of Science and Technology

<sup>3</sup>School of Materials Science and Engineering, Guilin University of Electronic Technology

<sup>4</sup>Molecular Photoscience Research Center, Kobe University

*(J. Phys.: Condens. Matter 26, 2014)*

High-field electron spin resonance measurements of an antiferromagnet  $\text{Ca}_3\text{ZnMnO}_6$  isostructure,

with the Ising-chain multiferroic  $\text{Ca}_3\text{ZnMnO}_6$ , have been carried out. Two distinct resonance modes were observed below  $T_N = 25$  K, which is well explained by conventional antiferromagnetic resonance theory with easy-plane anisotropy. The zero-field spin gap is derived to be about 166 GHz, originating from the easy-plane anisotropy and exchange interaction.

Our result suggests that the Dzyaloshinsky–Moriya interaction, which may induce spin canting, is absent. Disappearance of Ising anisotropy in  $\text{Ca}_3\text{ZnMnO}_6$  suggests that the  $\text{Co}^{4+}$  ion, as well as the Co–Mn superexchange, plays an important role for the Ising nature in  $\text{Ca}_3\text{ZnMnO}_6$ .

**Ground state of the spin-1/2 chain of green diopside at high fields**

**Kazuki Matsui, Masashi Fujisawa<sup>1</sup>, Kenta Hagiwara, Yukihiro Hoshino, Takayuki Goto\*, Takahiko Sasaki<sup>2</sup>, Hidekazu Tanaka<sup>3</sup>, Susumu Okubo<sup>1</sup>, and Hitoshi Ohta<sup>1</sup>**

Physics Division, Sophia University

<sup>1</sup>Molecular Photoscience Research Center, Kobe University

<sup>2</sup>Institute for Materials Research, Tohoku University,

<sup>3</sup>Department of Physics, Tokyo Institute of Technology

*(JPS Conf Proc 3, 2014)*

The gem-stone diopside  $\text{Cu}_6\text{Si}_6\text{O}_{18}\cdot 6\text{H}_2\text{O}$  has a chiral crystal structure of equilateral triangular helices consisting of Cu-3d spins. It shows an antiferromagnetic order with an easy axis along  $c$  at  $T_N = 14.5$  K under zero field, and a magnetization jump at  $HC = 13.5$  T when the field is applied along  $c$ -axis. By  $^{29}\text{Si}$ -NMR measurements, we have revealed that the high-field state is essentially the two sub-lattice structure, and that the component within  $ab$ -plane is collinear. The result indicates no apparent match with the geometrical pattern of helical spin chain.

### III-B. ESR, PL AND MAGNETIC PROPERTY MEASUREMENTS OF MAGNETIC SEMICONDUCTORS

Rare-earth ions incorporated in semiconductors show the luminescence originated from intra-4f-shell transition under electrical excitation or photo excitation of the host semiconductor. Especially, as the wavelength 1.5  $\mu\text{m}$  lies in the minimum loss region of silica fibers, the photoluminescence (PL) from  $\text{Er}^{3+}$  is very important for applications. ESR measurements have been performed intensively in order to clarify the functionality of various Er centers in GaAs:Er,O systems. Especially, we have shown that the Er-concentration dependence of intensities of ESR absorption has a strong correlation with the Er-concentration dependence of the photoluminescence (PL) intensities of GaAs:Er,O doped with carriers. The doping effect turns out to be similar to the effect of Zn doping. The analyses of ESR suggest the existence of exchange interaction between Er sites. This work is in close collaboration with Fujiwara group of Faculty of Engineering, Osaka University. We have proposed a model for the PL and ESR results and Fatma Elmasry received a Doctor Degree in March, 2015, for this work.

GdN thin film is studied by ESR, and the SQUID magnetometer described in III-D. SQUID measurements and the Arrott plot analyses revealed that the Curie temperature of the film is about 32 K. ESR measurements also showed clear ferromagnetic resonance (FMR) at 4.2 K and the analyses has been performed. This work is in close collaboration with Kita group of Faculty of Engineering, Kobe University. The paper by T. Shimokawa on FMR appeared in *J. Appl. Phys.*

#### **Electron spin resonance study of Er-concentration effect in GaAs:Er,O containing charge carriers**

**F. Elmasry<sup>1</sup>, S. Okubo<sup>2</sup>, H. Ohta<sup>1,2</sup>, and Y. Fujiwara<sup>3</sup>**

<sup>1</sup>Graduate School of Science, Kobe University

<sup>2</sup>Molecular Photoscience Research Center, Kobe University,

<sup>3</sup>Graduate School of Engineering, Osaka University

*(J. Appl. Phys. 115, 2014)*

Er-concentration effect in GaAs:Er,O containing charge carriers (n-type, high resistance, p-type) has been studied by X-band Electron spin resonance (ESR) at low temperature ( $4.7 \text{ K} < T < 18 \text{ K}$ ). Observed A, B, and C types of ESR signals were identical to those observed previously in

GaAs:Er,O without carrier. The local structure around Er-2O centers is not affected by carriers because similar angular dependence of g-values was observed in both cases (with/without carrier). For temperature dependence, linewidth and lineshape analysis suggested the existence of Er dimmers with antiferromagnetic exchange interaction of about 7K. Moreover, drastic decrease of ESR intensity for C signal in p-type sample was observed and it correlates with the decrease of photoluminescence (PL) intensity. Possible model for the Er-2O trap level in GaAs:Er,O is discussed from the ESR and PL experimental results.

## Electronic transitions in GdN band structure

R. Vidyasagar<sup>1</sup>, T. Kita<sup>1</sup>, T. Sakurai<sup>2</sup>, and H. Ohta<sup>3</sup>

<sup>1</sup>Department of Electrical and Electronic Engineering, Graduate School of Engineering, Kobe University

<sup>2</sup>Centre for Support to Research and Education Activities, Kobe University

<sup>3</sup>Molecular Photoscience Research Center and Graduate School of Science, Kobe University

(*J. Appl. Phys.* 115, 2014)

Using the near-infrared (NIR) absorbance spectroscopy, electronic transitions and spin polarization of the GdN epitaxial film have been investigated; and the GdN epitaxial film was grown by a reactive *rf* sputtering technique. The GdN film exhibited three broad bands in the NIR frequency regimes; and those bands are attributable primarily to the minority and majority spin transitions at the X-point and an indirect

transition along the  $\Gamma$ -X symmetric direction of GdN Brillouin zone.

We experimentally observe a pronounced red-shift of the indirect band gap when cooling down below the Curie temperature which is ascribed to the orbital-dependent coulomb interactions of Gd-*5dxy* electrons, which tend to push-up the N-2*p* bands. On the other hand, we have evaluated the spin polarization of 0.17 ( $\pm 0.005$ ), which indicates that the GdN epitaxial film has almost 100% spin-polarized carriers. Furthermore, the experimental result of GdN electronic transitions are consistent with the previous reports and are thus well-reproduced. The Arrott plots evidenced that the Curie temperature of GdN film is 36K and the large spin moment is explained by the nitrogen vacancies and the intra-atomic exchange interaction.

## Microscopic properties of degradation-free capped GdN thin films studied by electron spin resonance

Tokuro Shimokawa<sup>1</sup>, Yohei Fukuoka<sup>2</sup>, Masashi Fujisawa<sup>3</sup>, Weimin Zhang<sup>4</sup>, Susumu Okubo<sup>4</sup>, Takahiro Sakurai<sup>5</sup>, Hitoshi Ohta<sup>4</sup>, Reddithota Vidyasagar<sup>6</sup>, Hiroaki Yoshitomi<sup>6</sup>, Shinya Kitayama<sup>6</sup>, and Takashi Kita<sup>6</sup>

<sup>1</sup>Center for Collaborative Research and Technology Development, Kobe University

<sup>2</sup>Graduate School of Science, Kobe University

<sup>3</sup>Research Center for Low Temperature Physics, Tokyo Institute of Technology

<sup>4</sup>Molecular Photoscience Research Center, Kobe University

<sup>5</sup>Center for Supports to Research and Education Activities, Kobe University

<sup>6</sup>Department of Electrical and Electronic Engineering, Graduate School of Engineering, Kobe University

(*J. Appl. Phys.* 117, 2015)

The microscopic magnetic properties of high-quality GdN thin films have been investigated by electron spin resonance (ESR) and ferromagnetic resonance (FMR) measurements. Detailed temperature dependence ESR measurements have shown the existence of two ferromagnetic components at lower temperatures, which was not clear from the previous magnetization measurements. The temperature, where the resonance shift occurs for the major ferromagnetic component, seems to be consistent with the Curie temperature obtained from the previous magnetization measurement. On the other

hand, the divergence of line width is observed around 57K for the minor ferromagnetic component. The magnetic anisotropies of GdN thin films have been obtained by the analysis of FMR

angular dependence observed at 4.2K. Combining the X-ray diffraction results, the correlation between the magnetic anisotropies and the lattice constants is discussed.

### III-C. DEVELOPMENTS OF MULTI-EXTREME ESR SYSTEM, SQUID ESR AND MICRO-CANTILEVER ESR

High frequency high field ESR measurement has many advantages compared with the conventional X-band ESR, for instance, the high spectral resolution, measurements beyond a magnetic phase transition, and the detection of spin systems that have a large zero-field splitting, which is not possible by X-band ESR. However, THz ESR has the limitation of sensitivity at the moment. Therefore, a new, highly sensitive detection technique for THz ESR compatible with a high magnetic field is required for its wide application, and we are developing the highly sensitive THz ESR system using the micro-cantilever. E. Ohmichi is working on the microfabrication of MEMS cantilever for micro-cantilever ESR and developed a high-sensitivity cantilever ESR system using a fiber-optic interferometer and a Faraday method. H. Ohta gave an invited presentations about the multi-extreme ESR system including SQUID ESR and micro-cantilever ESR at International Conferences “Magnetic Resonance: fundamental research and pioneering applications (MR-70)” (June 23-27, 2014, Kazan, Russia), “International Symposium Catalytic Systems for Chemical Energy Conversion” (July 23-25, 2014, Mülheim an der Ruhr, Germany), and CONIAPS XVII (January 16-18, 2015, Jaipur, India). The master course student A. Ishikawa received the Best Presentation Award for the Physics Master Course Presentation at Kobe University and the SEST Student Research Award. S. Okamoto received the APES Poster Award and Dr. Alexey Alfonsov received the IES Poster Award at APES-IES-SEST2014.

We are also developing SQUID ESR, whose detection method is a longitudinal ESR similar to the cantilever ESR, after the installation of SQUID magnetometer in 2010. This development is done by a close collaboration with Dr. T. Sakurai (Center for Supports to Research and Education Activities, Kobe University). Although the applied field is limited to 5 T, this is a very simple method to perform millimeter wave ESR. The advantage of SQUID ESR is that we can obtain the absolute value of ESR intensity in the unit of magnetization. We have shown that SQUID ESR can be also applicable to the ESR measurement under pressure, and the high pressure up to 1.5 GPa. Moreover, the pressure region is expanded to 2.7 GPa using the hybrid-type piston-cylinder pressure cell, and the transmission-type high-field ESR system is developed with the combination of this pressure cell and the cryogen-free 10 T superconducting magnet. The developments of transmission-type pressure cells are done by the collaboration with Prof. Uwatoko (ISSP, University of Tokyo). T. Sakurai gave an invited presentations related to SQUID ESR at the meeting of The Spectroscopical Society of Japan in Osaka in November, 2014. The master course student K. Kawasaki received the SEST Student Research Award for the related topic.

### III-D. MAGNETIZATION MEASUREMENTS USING SQUID MAGNETOMETER

The installation of SQUID magnetometer in 2010 by a Grant-in-Aid Creative Scientific Research “Development of properties and functionalities by precise control of rare-earth doping” (2007-2011, Prof. Y. Fujiwara (Osaka University)) opened up wide varieties of collaborative researches. In 2014 users of SQUID magnetometer are Mochida and Takahashi groups, Uchino group, and Eda group (Department of Chemistry, Kobe University), Sugawara and Matsuoka group (Department of Physics, Kobe University), Kita group (Faculty of Engineering, Kobe University), Hasegawa group (ISIR, Osaka University), Kikuchi group (Department of Applied Physics, University of Fukui), T. Sakurai and S. Hara (Center for Supports to Research and Education Activities, Kobe University). It is also used for the development of SQUID ESR as described in III-C.

#### **Magnetic hysteresis behavior and magnetic pinning in a $d^0$ ferromagnet/superconductor nanostructure**

**T. Uchino<sup>1</sup>, Y. Uenaka<sup>1</sup>, H. Soma<sup>1</sup>, T. Sakurai<sup>2</sup>, and H. Ohta<sup>3</sup>**

<sup>1</sup>Department of Chemistry, Graduate School of Science, Kobe University

<sup>2</sup>Center for Support to Research and Education Activities, Kobe University

<sup>3</sup>Molecular Photoscience Research Center and Graduate School of Science, Kobe University  
(*J. Appl. Phys.* 115, 2014)

We investigate the interaction between superconductivity and defect-induced  $d^0$  ferromagnetism using a composite consisting of  $MgB_2$  and  $MgO$  nanocrystals. The composite exhibits a ferromagnetic hysteresis behavior in the temperature region from 40 to 300K. Defective  $MgO$  nanocrystals ( $\sim 20$  nm) embedded in the composite are considered to be responsible for the observed ferromagnetism. The zero field cool and field cool magnetization curves show that the superconducting transition occurs at  $T_c = 38.6$  K, in agreement with  $T_c$  of pure  $MgB_2$ . In the

temperature region from  $T_c$  to  $0.9T_c$  ( $\sim 35$  K), the magnetization hysteresis curves show a superposition of ferromagnetic (F) and superconducting (S) signals. When the temperature of the system is decreased below  $0.65T_c$  ( $\sim 25$ K), the S signals dominate over the F signals. The resulting magnetic hysteresis loops are highly asymmetric and the descending field branch is nearly flat, as predicted in the case of surface pinning. At temperatures below  $0.5T_c$  ( $\sim 20$ K), a sharp peak is developed near zero field in the magnetization hysteresis curves, implying an enhancement of superconducting vortex pinning. The observed pinning enhancement most likely results from magnetic pinning due to randomly distributed magnetic  $MgO$  grains, which yield the magnetic inhomogeneity and the related pinning potential in a length scale of  $\sim 100$  nm. Thus, the present ferromagnetic/superconducting composite provides an ideal model system that demonstrates the availability of  $d^0$  ferromagnetism as a source of magnetic potential for effective vortex pinning.

**Decamethyl- and octamethyl-ferrocenium salts of F<sub>1</sub>- and F<sub>2</sub>-TCNQ: Effects of fluorine substitution on the crystal structures and magnetic interactions**

**Y. Funasako<sup>1</sup>, T. Mochida<sup>1</sup>, T. Akasaka<sup>1,2</sup>, T. Sakurai<sup>3</sup>, H. Ohta<sup>4</sup>, Y. Nishio<sup>5</sup>**

<sup>1</sup>Department of Chemistry, Graduate School of Science, Kobe University

<sup>2</sup>Department of Chemistry, Faculty of Science, Toho University

<sup>3</sup>Center for Supports to Research and Education Activities, Kobe University

<sup>4</sup>Molecular Photoscience Research Center, Kobe University

<sup>5</sup>Department of Physics, Faculty of Science, Toho University

(*Inorganica Chimica Acta* 419, 2014)

Decamethyl- and octamethyl-ferrocenium salts of F<sub>n</sub>TCNQ (*n* = 1, 2) were prepared and their crystal

structures characterized. The 2,5-F<sub>2</sub>TCNQ salts [Fe(C<sub>5</sub>Me<sub>5</sub>)<sub>2</sub>](2,5-F<sub>2</sub>TCNQ) (1) and [Fe(C<sub>5</sub>Me<sub>4</sub>H)<sub>2</sub>](2,5-F<sub>2</sub>TCNQ) (2) exhibit one-dimensional [D]<sup>+</sup>[A]<sup>-</sup>[D]<sup>+</sup>[A]<sup>-</sup> mixed-stack structures, while the salts with polar acceptors [Fe(C<sup>5</sup>Me<sup>5</sup>)<sub>2</sub>][A] (A = F<sub>1</sub>TCNQ (3), 2,3-F<sub>2</sub>TCNQ (4), 2,6-F<sub>2</sub>TCNQ (5)) and [Fe(C<sub>5</sub>Me<sub>4</sub>H)<sub>2</sub>][A] (A = 2,3-F<sub>2</sub>TCNQ (6), 2,6-F<sub>2</sub>TCNQ (7)) consist of [D]<sup>+</sup>[A<sub>2</sub>]<sup>2-</sup>[D]<sup>+</sup> units involving a diamagnetic dimer of the acceptors. These salts are isomorphous to the corresponding TCNQ salts. 1 and 2 exhibit small ferromagnetic interactions at low temperatures. 1 undergoes an antiferromagnetic phase transition at *T*<sub>N</sub> = 3.9 K, which is higher than *T*<sub>N</sub> = 2.1 K of the metamagnetic polymorph of [Fe(C<sub>5</sub>Me<sub>5</sub>)<sub>2</sub>](TCNQ).

**Unusual Magnetic Phase Transition of 2D Kagomé Compound Cu<sub>3</sub>(CO<sub>3</sub>)(bpe)<sub>3</sub>2ClO<sub>4</sub>**

**H. Kikuchi<sup>1</sup>, Y. Fujii<sup>2</sup>, H. Nakata<sup>1</sup>, T. Taniguchi<sup>3</sup>, W. Zhang<sup>4</sup>, S. Okubo<sup>4</sup>, H. Ohta<sup>4</sup>**

<sup>1</sup>Department of Applied Physics, University of Fukui

<sup>2</sup>Research Center for Development of Far-Infrared Region, University of Fukui

<sup>3</sup>Graduate School of Science, Osaka University

<sup>4</sup>Molecular Photoscience Research Center, Kobe University

(*JPS Conf. Proc.* 3, 2014)

Cu<sub>3</sub>(CO<sub>3</sub>)(bpe)<sub>3</sub> · 2ClO<sub>4</sub> (bpe = 1,2-bis(4-pyridyl)ethane) is a two dimensional geometrically frustrated magnet with an *S*=1/2

slightly distorted kagomé lattice. We measured dc magnetization, ac magnetic susceptibility, field dependence of the specific heat, nuclear magnetic resonance (NMR) and electron spin resonance (ESR) spectra of powder sample of this compound to investigate its magnetic properties in detail. Although dc and ac magnetization data suggest the occurrence of ferromagnetic order at approximately 8 K, no anomaly in specific heat was observed at this temperature. The <sup>1</sup>H-NMR spectra of the sample drastically broaden at temperatures below approximately 10 K, suggesting the rapid development of internal magnetic field. Furthermore, the high field ESR spectra show anomalies below approximately 20 K. Contrary to conventional

magnetic transitions, the magnetic transition in this compound is not accompanied by a distinct anomaly

of specific heat. We have discussed possible reasons for the non-observance of specific heat anomaly.

**A biferrocenium salt containing paramagnetic tetracyanoquinodimethane hexamers: Charge disproportionation via donor-acceptor interaction**

**T. Mochida<sup>1</sup>, Y. Funasako<sup>1,2</sup>, K. Takahashi<sup>1</sup>, M. Inokuchi<sup>2</sup>, T. Sakurai<sup>3</sup>, S. Ikeda<sup>4</sup>, H. Ohta<sup>5</sup>, H. Mori<sup>6</sup>, M. Uruichi<sup>7</sup>**

<sup>1</sup>Department of Chemistry, Graduate School of Science, Kobe University

<sup>2</sup>Department of Applied Chemistry, Faculty of Engineering, Tokyo University of Science

<sup>3</sup>Center for Supports to Research and Education Activities, Kobe University

<sup>4</sup>Department of Physics, Graduate School of Science, Kobe University

<sup>5</sup>Molecular Photoscience Research Center, Kobe University

<sup>6</sup>Institute for Solid State Physics, The University of Tokyo

<sup>7</sup>Institute for Molecular Science

(*Chem. Commun.*, 50, 2014)

Crystal engineering of mixed valence compounds has been a topic of continuous interest for many

years. Biferrocene is an electron donor (D) comprised of two ferrocene units exhibiting both mixedvalence monocation ( $D^+$ ) and non-mixed-valence dication ( $D^{2+}$ ) oxidation states. To date, many biferrocenium salts containing  $D^+$  have been prepared, and their valence states have been extensively investigated. Recently, we prepared a series of alkyl-biferrocenium salts with various acceptor (A) molecules, including tetracyanoquinodimethane (TCNQ) derivatives. Salts with D/A ratios of 1 : 1–1 : 3 were obtained; the valency of the donor changes from  $D^+$  to  $D^{2+}$  with increasing stoichiometry. In particular, the intermediate salts contain both  $D^{2+}$  and  $D^+$  molecules. The coexistence of dications and monocations is an interesting phenomenon that has also been found in viologen salts. Charge disproportionation, or charge separation, is an important topic in the physics of charge transfer salts.

## Original Papers

## 発表論文

authors	title	journal	Vol.	page	year
Hiroshi Anzai, Neeraj Kumar Joshi, Mazanori Fuyuki, Akihide Wada	Fourier Transform Two-dimensional Fluorescence Excitation Spectrometer (FT-2DFES) by using Tandem Fabry-Pérot Interferometer	<i>Rev. Sci. Inst.</i>	<b>86</b>	14101	2015
K. Tada, W. Kashihara, M. Baba, T. Ishiwata, E. Hirota, and S. Kasahara	High-resolution laser spectroscopy and magnetic effect of the $B^2E' \leftarrow X^2A_2'$ transition of $^{14}\text{NO}_3$ radical	<i>J. Chem. Phys.</i>	<b>141</b>	184307	2014
K. Tada, K. Teramoto, T. Ishiwata, E. Hirota, and S. Kasahara	High-resolution laser spectroscopy and magnetic effect of the $B^2E' \leftarrow X^2A_2'$ transition of the $^{15}\text{N}$ substituted nitrate radical	<i>J. Chem. Phys.</i>		in press	
Yusuke Iima, Daiki Kuzuhara, Zhao-Li Xue, Seiji Akimoto, Hiroko Yamada, and Keisuke Tominaga	Time-Resolved Fluorescence Spectroscopy Study of Excited State Dynamics of Alkyl- and Benzo-Substituted Triphyrin(2.1.1)	<i>Phys. Chem. Chem. Phys.</i>	<b>16</b>	13129 – 13135	2014
Feng Zhang, Michitoshi Hayashi, Houg-Wei Wang, Keisuke Tominaga, Ohki Kambara, Jun-ichi Nishizawa, and Tetsuo Sasaki	Terahertz spectroscopy and solid-state density functional theory calculation of anthracene: effect of dispersion force on the vibrational modes	<i>J. Chem. Phys.</i>	<b>140</b>	174509	2014
Yuki Fukui, Kaoru Ohta, and Keisuke Tominaga	Vibrational Dynamics of the CO Stretching of 9-Fluorenone Studied by Visible-pump and Infrared-probe Spectroscopy	<i>Faraday Discussion</i>		in press	
Naoki Yamamoto, Tomoyo Andachi, Atsuo Tamura, and Keisuke Tominaga	Temperature and hydration dependence of low-frequency spectra of lipid bilayers studied by terahertz time-domain spectroscopy	<i>J. Phys. Chem. B</i>		in press	
Feng Zhang, Houg-Wei Wang, Keisuke Tominaga, and Michitoshi Hayashi	Intramolecular Vibrations in Low-Frequency Normal Modes of Amino Acids: L-Alanine in Neat Solid State	<i>J. Phys. Chem. A</i>		in press	
R. Nagao, M. Yokono, A. Teshigahara, S. Akimoto, T. Tomo	Light-harvesting ability of the fucoxanthin chlorophyll a/c-binding protein associated with photosystem II from the diatom <i>Chaetoceros gracilis</i> as revealed by picosecond time-resolved fluorescence spectroscopy	<i>J. Phys. Chem. B</i>	<b>118</b>	5093-5100	2014
R. Hayashi, G. Shimakawa, K. Shaku, S. Shimizu, S. Akimoto, H. Yamamoto, K. Amako, T. Sugimoto, M. Tamoi, A. Makino, C. Miyake	$\text{O}_2$ -dependent large electron flow functions as electron sink, replacing the steady-state electron flux in photosynthesis in the cyanobacterium <i>Synechocystis</i> sp. PCC 6803, but not in the cyanobacterium <i>Synechococcus</i> sp. PCC 7942	<i>Biosci. Biotech. Biochem.</i>	<b>78</b>	384-393	2014
S. Akimoto, M. Yokono, E. Yokono, S. Aikawa, A. Kondo	Short-term light adaptation of a cyanobacterium, <i>Synechocystis</i> sp. PCC 6803, proved by time-resolved fluorescence spectroscopy	<i>Plant Physiol. Biochem.</i>	<b>81</b>	149-154	2014
M. Araki, S. Akimoto, M. Mimuro, T. Tsuchiya	Artificially acquired chlorophyll <i>b</i> is highly acceptable to the thylakoid-lacking cyanobacterium, <i>Gloeobacter violaceus</i> PCC 7421	<i>Plant Physiol. Biochem.</i>	<b>81</b>	155-162	2014

T. Tomo, T. Shinoda, M. Chen, S. I. Allakhverdiev, S. Akimoto	Energy transfer processes in chlorophyll <i>f</i> -containing cyanobacteria using time-resolved fluorescence spectroscopy on intact cells	<i>Biochim. Biophys. Acta</i>	<b>1837</b>	1484-1489	2014
S. Akimoto, A. Teshigahara, M. Yokono, M. Mimuro, R. Nagao, T. Tomo	Excitation relaxation dynamics and energy transfer in fucoxanthin-chlorophyll <i>a/c</i> -protein complexes, probed by time-resolved fluorescence	<i>Biochim. Biophys. Acta</i>	<b>1837</b>	1514-1521	2014
H. Yamamoto, K. Ohkubo, S. Akimoto, S. Fukuzumi, A. Tsuda	Control of reaction pathways in the photochemical reaction of a quinone with tetramethylethylene by metal binding	<i>Org. Bio. Chem.</i>	<b>36</b>	7004-7017	2014
R. Nagao, M. Yokono, T. Tomo, S. Akimoto	Control mechanism of excitation energy transfer in a complex consisting of photosystem II and fucoxanthin chlorophyll <i>a/c</i> -binding protein	<i>J. Phys. Chem. Lett</i>	<b>5</b>	2983-2987	2014
Y. Ueno, S. Aikawa, A. Kondo, S. Akimoto	Light adaptation of the unicellular red alga, <i>Cyanidioschyzon merolae</i> , probed by time-resolved fluorescence spectroscopy	<i>Photosynth. Res.</i>		in press	
K. Niki, S. Aikawa, M. Yokono, A. Kondo, S. Akimoto	Differences in energy transfer of a cyanobacterium, <i>Synechococcus</i> sp. PCC 7002, grown in different cultivation media	<i>Photosynth. Res.</i>		in press	
M. Iwai, M. Yokono, M. Kondo, K. Noguchi, S. Akimoto, A. Nakano	Light-harvesting complex Lhcb9 confers a green alga-type photosystem I supercomplex to the moss <i>Physcomitrella patens</i>	<i>Nature Plants</i>		in press	
A. Onishi, S. Aikawa, A. Kondo, S. Akimoto	Energy transfer in <i>Anabaena variabilis</i> filaments under nitrogen depletion, studied by time-resolved fluorescence	<i>Photosynth. Res.</i>		in press	
S. Akimoto, T. Shinoda, M. Chen, S. I. Allakhverdiev, T. Tomo	Energy transfer in the chlorophyll <i>f</i> -containing cyanobacterium, <i>Halomicronema hongdechloris</i> , analyzed by time-resolved fluorescence spectroscopies	<i>Photosynth. Res.</i>		in press	
M. Yokono, A. Takabayashi, S. Akimoto, A. Tanaka	A megacomplex composed of both photosystem reaction centers in higher plants	<i>Nature Communications</i>		accepted	
T. Uchino, Y. Uenaka, H. Soma, T. Sakurai, and H. Ohta	Magnetic hysteresis behavior and magnetic pinning in a $d^0$ ferromagnet/superconductor nanostructure	<i>J. Appl. Phys.</i>	<b>115</b>	063910/1-8	2014
F. Elmasry, S. Okubo, H. Ohta, and Y. Fujiwara	Electron spin resonance study of Er-concentration effect in GaAs;Er,O containing charge carriers	<i>J. Appl. Phys.</i>	<b>115</b>	193904/1-7	2014
R. Vidyasagar, T. Kita, T. Sakurai, and H. Ohta	Electronic transitions in GdN band structure	<i>J. Appl. Phys.</i>	<b>115</b>	203717/1-5	2014
Y. Funasako, T. Mochida, T. Akasaka, T. Sakurai, H. Ohta, Y. Nishio	Decamethyl- and octamethyl-ferrocenium salts of F1- and F2-TCNQ: Effects of fluorine substitution on the crystal structures and magnetic interactions	<i>Inorganica Chimica Acta</i>	<b>419</b>	105-110	2014
M Y Ruan, Z W Ouyang, Y M Guo, J J Cheng, Y C Sun, Z C Xia, G H Rao, S Okubo and H Ohta	Disappearance of Ising nature in $\text{Ca}_3\text{ZnMnO}_6$ studied by high-field ESR	<i>J. Phys.: Condens. Matter</i>	<b>26</b>	236001/1-5	2014

K. Matsui, M. Fujisawa, K. Hagiwara, Y. Hoshino, T. Goto, T. Sasaki, H. Tanaka, S. Okubo and H. Ohta	Ground state of the spin-1/2 chain of green diopside at high fields	<i>JPS Conf. Proc.</i>	<b>3</b>	014011/1-6	2014
H. Kikuchi, Y. Fujii, H. Nakata, T. Taniguchi, W. Zhang, S. Okubo, H. Ohta	Unusual Magnetic Phase Transition of 2D Kagom'e Compound $\text{Cu}_3(\text{CO}_3)(\text{bpe})_32\text{ClO}_4$	<i>JPS Conf. Proc.</i>	<b>3</b>	012019	2014
T. Mochida, Y. Funasako, K. Takahashi, M. Inokuchi, T. Sakurai, S. Ikeda, H. Ohta, H. Mori, M. Uruichi	A biferrocenium salt containing paramagnetic tetracyanoquinodimethane hexamers: Charge disproportionation via donor-acceptor interactions	<i>Chem. Commun.</i>	<b>50</b>	13370-13372	2014
T. Shimokawa, Y. Fukuoka, M. Fujisawa, W. Zhang, S. Okubo, T. Sakurai, H. Ohta, R. Vidyasagar, H. Yoshitomi, S. Kitayama, and T. Kita	Microscopic properties of degradation-free capped GdN thin films studied by electron spin resonance	<i>J. Appl. Phys.</i>	<b>117</b>	043909	2015

## Invited Talks (domestic and international)

## 招待講演(国内および国際研究集会)

発表者氏名	開催時期	開催地	plenary or invite	学会名	講演題目
富永圭介 K. Tominaga	2014.4	Seoul, Korea	invite	5 <sup>th</sup> International THz-Bio Workshop	THz Spectroscopy on Condensed Matter: Molecular Crystals, Aqueous Solutions, and Proteins
	2014.8	Los Baños, Philippines	plenary	Symposium on Ultrafast Spectroscopy: Its applications on Life and Environmental Sciences	Terahertz Spectroscopy on Molecular Crystals
	2014.12	Kolkata, India	invite	Advances in Spectroscopy and Ultrafast Dynamics	Terahertz Spectroscopy on Condensed Matter; Molecular Crystals and Proteins
	2015.1	Bangalore, India	invite	Temporally and Spatially Resolved Molecular Science, Faraday Discussion 177	Vibrational Dynamics of the CO Stretching of 9-Fluorenone Studied by Visible-pump and Infrared-probe Spectroscopy
	2015.1	Bangalore, India	invite	Advances in Structure & Dynamics	Low-frequency Vibrational Motions of Condensed Phases Studied by Terahertz Time Domain Spectroscopy
	2015.1	Hamamatsu	invite	International Symposium toward the Future of Advanced Researches in Shizuoka University 2015	Terahertz spectroscopy on condensed matter
	2015.2	Taipei, Taiwan	invite	1 <sup>st</sup> Symposium for the Promotion of Applied Research collaboration in Asia (SPARCA 2015)	Characterization of Condensed Material by Terahertz Radiation Spectroscopy
	2015.3	Kolkata, India	invite	Asian Academic Seminar and School 2015	Terahertz Spectroscopy on Condensed Matter; Molecular Crystals and Proteins
近藤未菜子 M. Kondo	2014.8	Los Baños, Philippines	plenary	Symposium on Ultrafast Spectroscopy: Its applications on Life and Environmental Sciences	Dynamics of the H-Bond Complex Formation of the Excited State 4-Aminophthalimide Analogue studied by Time-Resolved Vibrational Spectroscopy
秋本誠志 S. Akimoto	2014.4	仙台	invite	理研シンポジウム「最先端光計測とライフサイエンスの近未来 -バイオ・ラマン2017- [4]」	光合成系における励起エネルギー移動の環境応答
	2014.5	奈良	invite	公開シンポジウム「多様な光合成の世界」、第5回日本光合成学会年会	クロロフィルの光エネルギー捕集にみられる多様性
	2014.6	Pushchino, Russia	invite	Photosynthesis Research for Sustainability – 2014	Differences in energy transfer of cyanobacteria grown in different cultivation media
	2014.7	名古屋	invite	光合成セミナー2014:反応中心と色素系の多様性	時間分解蛍光分光法を用いた光合成初期過程の観測
太田仁 H. Ohta	2014.5	八王子	invite	第9回 ESR 入門セミナー	ESR 超入門
	2014.5	八王子	invite	第9回 ESR 入門セミナー	ESR の基礎と原理
	2014.5	八王子	invite	第9回 ESR 入門セミナー	固体の ESR スペクトル解析法 (固体試料の ESR 測定から高分解能 ESR へ)
	2014.6	Kazan, Russia	invite	Magnetic Resonance: fundamental research and pioneering applications (MR-70)	Developments and applications of multi-extreme THzESR
	2014.7	愛知	invite	第12回 ESR 夏の学校	電子スピン共鳴 (ESR)序論

	2014.7	Mülheim an der Ruhr, Germany	invite	International Symposium Catalytic Systems for Chemical Energy Conversion	Multi-Extreme THz ESR Systems in Kobe
	2014.7	Toulouse, France	invite	Recent development of multi-extreme high field THz ESR and some applications (セミナー)	Recent development of multi-extreme high field THz ESR and some applications
	2015.1	Jaipur, India	invite	CONIAPS XVII	Developments and Applications of Multi-Extreme THz ESR Systems in Kobe
櫻井敬博 T. Sakurai	2014.11	大阪	invite	日本分光学会関西支部平成26年度最近の分光学の 進歩に関する講演会-最新 デバイスを用いた分光 法の進展-	SQUID 磁束計を用いた ESR 測定技術の 開発と圧力下測定への展開

Presentation at conferences (international and domestic)

一般講演

発表者氏名	開催時期	開催地	発表形態	学会名	講演題目
和田昭英	2014.6	姫路	poster	31 <sup>th</sup> Symposium on Chemical Kinetics and Dynamics	Observation of two-dimensional excitation spectrum using tandem Fabry-Perot interferometer
	2014.9	広島	poster	分子科学討論会	Fourier Transform Two Dimensional Excitation Spectrometer by using Tandem Fabry-Pérot Interferometer
笠原俊二	2014.6	Ohio, USA	oral	69 <sup>th</sup> International Symposium on Molecular Spectroscopy	Rotationally-resolved high-resolution laser spectroscopy of the B <sup>2</sup> E' ← X <sup>2</sup> A <sub>2</sub> ' transition of <sup>14</sup> NO <sub>3</sub> Radical
	2014.6	Potsdam, Germany	poster	23 <sup>rd</sup> International Conference on High Resolution Molecular Spectroscopy	High-resolution Laser spectroscopy of S <sub>1</sub> - S <sub>0</sub> transition of naphthalene and Cl-naphthalenes
富永圭介	2014.7	Lisbon, Portugal	poster	Liquids 2014 9 <sup>th</sup> Liquid Matter Conference	Vibrational Dynamics of Solute in Aqueous Solution Studied by Nonlinear Infrared Spectroscopy
	2014.7	Lisbon, Portugal	poster	Liquids 2014 9 <sup>th</sup> Liquid Matter Conference	Characterization of complex Dielectric Spectra of Aqueous Solutions with Ions from MHz to Mid Infrared Regions
	2014.9	Wisla, Poland	oral	8 <sup>th</sup> International Conference on Broadband Dielectric Spectroscopy and its Applications	Temperature and Hydration Dependence of Complex Dielectric Spectra of Lysozyme from GHz to THz Frequency Region
太田薫	2014.7	Okinawa, Japan	oral	19 <sup>th</sup> International Conference on Ultrafast Phenomena	Vibrational Dynamics of Nitrosyl Stretch of Ru Complex in Aqueous Solution Studied by Two-Dimensional Infrared Spectroscopy
秋本誠志	2014.10	Uppsala, Sweden	poster	12 <sup>th</sup> Nordic Photosynthesis Congress	Changes in light-harvesting and energy-transfer processes under different cultivation lights, probed by time-resolved fluorescence spectroscopy
	2015.3	東京	oral	第 56 回日本植物生理学会年会	Excitation energy transfer in thylakoid membranes from the chlorophyll <i>f</i> -containing cyanobacterium
太田仁	2014.5	大阪	oral	第 1 回西日本強磁場科学研究会プログラム	多重極限強磁場 THzESR の開発と KOFUC ネットワークの展望
	2014.6	Moscow, Russia	oral	Moscow International Symposium on Magnetism (MISM-2014)	High field ESR Study of frustrated antiferromagnets
	2014.7	Colorado, USA	oral	Rocky Mountain EPR Symposium	Multi-Extreme THz ESR: Present and Future.
	2014.8	Buenos Aires, Argentina	oral	27 <sup>th</sup> International Conference on Low Temperature Physics	Kagome lattice antiferromagnet Cr-Jarosite studied by high field ESR
	2014.11	奈良	poster	APES-IES-SEST 2014	Recent Development of Multi-Extreme THz ESR in Kobe
	2015.1	福井	oral	量子スピン系研究会	多重極限テラヘルツ ESR の進展と KOFUC ネットワーク
大道英二 (理学研究科)	2014.5	大阪	oral	第 1 回西日本強磁場科学研究会プログラム	カンチレバーを用いた超高感度 ESR 測定の現状と今後の展望
	2014.11	奈良	poster	APES-IES-SEST 2014	Recent advances in cantilever-detected ESR technique
	2014.12	大阪	oral	第 11 回強磁場フォーラム総会	KOFUC ネットワークに向けた高感度カンチレバー ESR 測定

	2015.3	東京	oral	日本物理学会 2015 年春季大会	バイメタルカンチレバーを用いた熱的検出高周波 ESR 測定法の開発
大久保晋	2014.5	大阪	oral	第一回西日本強磁場科学研究会プログラム	強磁場 THzESR によるスピン系の研究
	2014.9	愛知	oral	日本物理学会 2014 年秋季大会	スピネル化合物 $\text{GeCo}_2\text{O}_4$ の単結晶試料による ESR 測定 4
	2014.11	奈良	poster	APES-IES-SEST 2014	High-field ESR Measurements of Low-dimensional Magnets in Natural Minerals
	2014.12	大阪	poster	第 11 回強磁場フォーラム総会	$S=1/2$ 擬 1 次元フラストレート磁性体 $\text{NaCuMoO}_4(\text{OH})$ の強磁場 ESR 測定
	2015.1	福井	oral	量子スピン系研究会	新しい $S=1/2$ ハニカム格子反強磁性体? $\text{ScCu}_{2/3}\text{V}_{1/3}\text{O}_3$ の強磁場 ESR 測定
	2015.3	東京	oral	日本物理学会 2015 年春季大会	$\text{YCrO}_3$ の高周波 ESR 測定 2
櫻井敬博 (研究基盤センター)	2014.5	大阪	oral	第 1 回西日本強磁場科学研究会プログラム	圧力下強磁場 ESR の現状と展望
	2014.9	愛知	oral	日本物理学会 2014 年秋季大会	圧力下強磁場多周波数 ESR 装置の高感度化と応用
	2014.11	奈良	poster	APES-IES-SEST 2014	Development of High Pressure and Multi-frequency ESR System and Its Application to Quantum Spin System
	2014.12	大阪	poster	第 1 1 回強磁場フォーラム総会	高圧下テラヘルツ強磁場 ESR の開発と KOFUC ネットワークへの展開
	2015.3	東京	poster	日本物理学会 2015 年春季大会	圧力下強磁場多周波数 ESR 装置の高感度化と応用 II
原茂生 (研究基盤センター)	2014.9	愛知	oral	日本物理学会 2014 年秋季大会	新規 Co 系 1 次元鎖酸化物の構造と磁性
	2014.11	奈良	poster	APES-IES-SEST 2014	Magnetic Anisotropy of the Distorted-Diamond-Chain Compound $\text{Cu}_3(\text{MoO}_4)_2(\text{OH})_2$
	2015.3	東京	poster	日本物理学会 2015 年春季大会	水熱合成による単結晶 $\text{M}_2\text{CoGe}_2\text{O}_7$ の単結晶育成と磁化の異方性測定

Presentation by Graduate Students and Postdocs

院生、ポストドクの学会発表

指導教員	発表者氏名	学年	時期	学会名	講演題目
和田昭英 A. Wada	Neeraj Kumar Joshi	PD	2014.6	31 <sup>th</sup> Symposium on Chemical Kinetics and Dynamics	Polarity Controlled Reaction Path and Kinetics of Thermal Cis-to-Trans Isomerization of 4-Aminoazobenzene
	Neeraj Kumar Joshi	PD	2014.9	第 8 回分子科学討論会	On the Branching Ratio of Photoisomerization of 4-Aminoazobenzene
笠原俊二 S. Kasahara	多田康平	D3	2014.5	第 14 回分子分光研究会	<sup>15</sup> NO <sub>3</sub> ラジカルの B-X 遷移 0-0 バンドの高分解 能レーザー分光
	中野拓海	D3	2014.5	第 14 回分子分光研究会	ナフタレンの S <sub>1</sub> 状態の高振動状態の高分解能 レーザー分光
	山本涼	M2	2014.5	第 14 回分子分光研究会	単一モード紫外レーザーによるクロロナフタレン の高分解能分光
	多田康平	D3	2014.6	30 <sup>th</sup> Symposium on Chemical Kinetics and Dynamics	High-resolution Laser Spectroscopy of the B-X Transition of Nitrate Radical
	中野拓海	D3	2014.6	30 <sup>th</sup> Symposium on Chemical Kinetics and Dynamics	High-resolution UV laser spectroscopy of vibronic bands of naphthalene S <sub>1</sub> - S <sub>0</sub> transition
	山本涼	M2	2014.6	30 <sup>th</sup> Symposium on Chemical Kinetics and Dynamics	High-resolution UV Laser spectroscopy of S <sub>1</sub> - S <sub>0</sub> transition of chloronaphthalene
	多田康平	D3	2014.6	69 <sup>th</sup> International Symposium on Molecular Spectroscopy	Rotationally-resolved high-resolution laser spectroscopy of the B <sup>2</sup> E' ← X <sup>2</sup> A <sub>2</sub> ' Transition of <sup>15</sup> NO <sub>3</sub> Radical
	多田康平	D3	2014.9	23 <sup>rd</sup> International Conference on High Resolution Molecular Spectroscopy	Rotationally-resolved high-resolution Laser spectroscopy of <sup>15</sup> NO <sub>3</sub> Radical
	多田康平	D3	2014.9	第 8 回分子科学討論会	<sup>15</sup> NO <sub>3</sub> ラジカルの B-X 遷移の高分解能レーザー 分光
	中野拓海	D3	2014.9	第 8 回分子科学討論会	ナフタレン S <sub>1</sub> -S <sub>0</sub> 遷移の振電バンドにおける高分 解能レーザー分光
	山本涼	M2	2014.9	第 8 回分子科学討論会	クロロナフタレンの S <sub>1</sub> ←S <sub>0</sub> 遷移の高分解能レー ザー分光～振動励起状態の観測～
	多田康平	D3	2014.11	Indo-Japan Joint Workshop on "Frontiers in Molecular Spectroscopy: Fundamentals and Applications to Material and Biology"	High-resolution laser spectroscopy and Zeeman effect of free radical NO <sub>3</sub>
富永圭介 K. Tominaga	平岡翔	M2	2014.7	19 <sup>th</sup> International Conference on Ultrafast Phenomena	Vibrational Dynamics of the CN Stretching in the Electronically Excited State by UV and Visible-Pump and Infrared-Probe Spectroscopy
	奥田真紀	D1	2014.7	Gordon research conference "Water and Aqueous Solution"	The Dynamics of Non-ionic Molecules in Aqueous Solution Studied by Two-dimensional Infrared Spectroscopy
	近藤未菜子	PD	2014.7	Gordon research conference "Water and Aqueous Solution"	Hydrogen Bonding Interaction between Acetate Anion and Water Molecule: Influence of cations
	近藤未菜子	PD	2014.8	Symposium on Ultrafast Spectroscopy: Its applications on Life and Environmental Sciences	Dynamics of the H-Bond Complex Formation of the Excited State 4-Aminophthalimide Analogue studied by Time-Resolved Vibrational Spectroscopy

岡田梨沙	M2	2014.9	第8回分子科学討論会	テラヘルツ時間領域分光法によるトレハロースにコートされたリゾチームの低振動ダイナミクス
松苗康德	M2	2014.9	第8回分子科学討論会	時間分解蛍光分光法による凝集誘起発光の機構に関する研究
難波英里	M1	2014.9	第8回分子科学討論会	20 MHz から 4000 cm <sup>-1</sup> における分光学的測定によるグアニジウムイオンと水の相互作用
近藤未菜子	PD	2014.9	第8回分子科学討論会	超高速時間分解赤外分光法による水素結合錯体の振動ダイナミクス
奥田真紀	D1	2014.9	第8回分子科学討論会	二次元赤外分光法による水溶液中における非イオン性振動プローブ分子の動的挙動
平岡翔	M2	2014.9	第8回分子科学討論会	光ポンプ-テラヘルツプローブ分光装置の開発とその電荷キャリアダイナミクスへの応用
Feng Zhang	PD	2014.9	第8回分子科学討論会	Phonon Modes of Molecular Crystals Studied by Terahertz Spectroscopy and Solid-state Density Functional Theory; a Concept of Vibrational Coordinate Distribution
Feng Zhang	PD	2014.1	SPIE Photonics Asia	Low-frequency vibration study of amino acids using terahertz spectroscopy and solid-state density functional theory
奥田真紀	D1	2014.11	Indo-Japan Joint Workshop on "Frontiers in Molecular Spectroscopy: Fundamentals and Applications to Material and Biology	Vibrational Dynamics of Non-Ionic Molecules in Aqueous Solution Studied by Two-Dimensional Infrared Spectroscopy
岡田梨沙	M2	2014.12	Advances in Spectroscopy and Ultrafast Dynamics	Low-frequency dynamics of trehalose-coated lysozyme studied by terahertz time-domain spectroscopy
難波英里	M1	2014.12	若手フロンティア研究会 2014	広帯域分光測定によるグアニジウムイオンと水との相互作用
奥田真紀	D1	2015.1	神戸大学先端融合科学シンポジウム『生体分子のダイナミクスを眺める』	二次元赤外分光法による水溶液中における非イオン性振動プローブ分子の動的挙動
平岡翔	M2	2015.1	神戸大学先端融合科学シンポジウム『生体分子のダイナミクスを眺める』	光ポンプ-テラヘルツプローブ分光装置の開発とその電荷キャリアダイナミクスへの応用
松苗康德	M2	2015.1	神戸大学先端融合科学シンポジウム『生体分子のダイナミクスを眺める』	時間分解蛍光分光法による凝集誘起発光の機構に関する研究
岡田梨沙	M2	2015.1	神戸大学先端融合科学シンポジウム『生体分子のダイナミクスを眺める』	Low-frequency Dynamics of Trehalose-coated Lysozyme Studied by Terahertz Time-Domain Spectroscopy
難波英里	M1	2015.1	神戸大学先端融合科学シンポジウム『生体分子のダイナミクスを眺める』	広帯域分光測定によるグアニジウムイオンと水との相互作用
Feng Zhang	PD	2015.1	神戸大学先端融合科学シンポジウム『生体分子のダイナミクスを眺める』	Intramolecular Vibrations in Low-Frequency Normal Modes of Amino Acids: L-Alanine in Neat Solid Stat

	奥田真紀	D1	2015.3	Asian Academic Seminar and School 2015	Vibrational Dynamics on Non-Ionic Molecules in Aqueous Solution Studied by Two-Dimensional Infrared Spectroscopy
秋本誠志 S. Akimoto	大西亜弥	M1	2014.6	Photosynthesis Research for Sustainability – 2014	Energy transfer in <i>Anabaena variabilis</i> filaments during heterocyst differentiation studied by time-resolved fluorescence
	植野嘉文	M1	2014.6	Photosynthesis Research for Sustainability – 2014	Light adaptation of the primitive red alga <i>Cyanidioschyzon merolae</i> , proved by time-resolved fluorescence spectroscopy
	高下友基	M2	2014.7	光合成セミナー2014：反応中心と色素系の多様性	異なる色素組成をもつフィコビリソームにおける励起エネルギー移動過程
	大西亜弥	M1	2014.7	光合成セミナー2014：反応中心と色素系の多様性	時間分解蛍光分光法を用いた <i>Anabaena variabilis</i> の窒素欠乏条件下におけるエネルギー移動過程の観測
	植野嘉文	M1	2014.7	光合成セミナー2014：反応中心と色素系の多様性	異なる光質下で培養された紅藻 <i>Cyanidioschyzon merolae</i> のエネルギー移動過程
	植野嘉文	M1	2014.12	若手フロンティア研究会 2014	原始紅藻 <i>Cyanidioschyzon merolae</i> のエネルギー移動の培養光質依存性
	大西亜弥	M1	2014.12	若手フロンティア研究会 2014	窒素欠乏条件下における励起エネルギー移動過程の変化
	大西亜弥	M1	2015.3	第56回日本植物生理学会年会	Energy transfer changes in <i>Anabaena variabilis</i> filaments under nitrogen depletion
	植野嘉文	M1	2015.3	第56回日本植物生理学会年会	Long-term light adaptation of the unicellular red alga <i>Cyanidioschyzon merolae</i> , probed by time-resolved fluorescence spectroscopy
太田仁 H. Ohta	吉田翔太	M1	2014.9	日本物理学会 2014 年秋季大会	2次元反強磁性体 $Sr_2MO_3X$ ( $M=Cr, Ni$ $X=F, Cl$ ) の強磁場 ESR 測定
	北原遥子	M1	2014.9	日本物理学会 2014 年秋季大会	擬1次元プラストレート磁性体 $NaCuMoO_4(OH)$ の強磁場 ESR 測定
	川崎航平	M1	2014.9	日本物理学会 2014 年秋季大会	マイクロコイルを用いた圧力下での ESR 測定装置の開発
	荒川翔	M2	2014.9	日本物理学会 2014 年秋季大会	$CuB_2O_4$ の ESR による研究
	松井亮輔	M2	2014.9	日本物理学会 2014 年秋季大会	圧力下サイクロトロン共鳴装置の開発とディラック電子系への応用
	池田将平	M2	2014.9	日本物理学会 2014 年秋季大会	$YCrO_3$ とその関連物質における強磁場 ESR 測定
	肘井敬吾	PD	2014.9	日本物理学会 2014 年秋季大会	4体相互作用を持つ $S=1/2$ 量子スピン梯子系における基底状態相図についての数値的研究
	F. Elmasry	D3	2014.11	APES-IES-SEST 2014	Er-concentration and charge carrier effects on GaAs:Er,O revealed by X-band ESR
	松井亮輔	M2	2014.11	APES-IES-SEST 2014	Development of High Pressure Cyclotron Resonance Systems and Application to Dirac Fermion System
	川崎航平	M1	2014.11	APES-IES-SEST 2014	Development of high pressure ESR systems using micro-coil
	岡本翔	M1	2014.11	APES-IES-SEST 2014	Application of cantilever-detected ESR to biological systems
	石川陽帆	M2	2014.11	APES-IES-SEST 2014	High sensitive force detection system for high-frequency ESR measurement
	田伏諒	M2	2014.11	APES-IES-SEST 2014	Cantilever-detected ESR measurement using a frequency modulation technique
Alexey Alfonsov	PD	2014.11	APES-IES-SEST 2014	High Frequency ferromagnetic resonance study of Heusler Compounds using a micro-cantilever	

荒川翔	M2	2014.11	APES-IES-SEST 2014	Magnetic Anisotropy in Chiral System $\text{CuB}_2\text{O}_4$ by ESR
吉田翔太	M1	2014.11	APES-IES-SEST 2014	High Field ESR Measurements of Two Dimensional Antiferromagnets $\text{Sr}_2\text{NiO}_3\text{X}$ (X=F, Cl)
北原遥子	M1	2014.11	APES-IES-SEST 2014	High Field ESR Measurements of Quasi One Dimensional Frustrated Magnet $\text{NaCuMoO}_4(\text{OH})$
池田将平	M2	2014.11	APES-IES-SEST 2014	High-field ESR Measurements of $\text{YCrO}_3$ and $\text{YCaCrO}_4$
肘井敬吾	PD	2014.11	APES-IES-SEST 2014	Numerical study of dynamical susceptibility in one dimensional trimerized spin systems
吉田翔太	M1	2014.11	日本赤外線学会 第 24 回 研究発表会	2次元反強磁性体 $\text{Sr}_2\text{NiO}_3\text{X}$ (X=F,Cl)のテラヘルツ ESR 測定
北原遥子	M1	2014.11	日本赤外線学会 第 24 回 研究発表会	擬一次元プラスとレート磁性体 $\text{NaCuMoO}_4(\text{OH})$ のテラヘルツ ESR 測定
池田将平	M2	2014.11	日本赤外線学会 第 24 回 研究発表会	ペロブスカイト化合物 $\text{YCrO}_3$ のテラヘルツ ESR 測定
岡本翔	M1	2014.11	日本赤外線学会 第 24 回 研究発表会	カンチレバーを用いた高分解能生体 ESR 測定に向けた試み
田伏諒	M2	2014.11	日本赤外線学会 第 24 回 研究発表会	バイメタル構造を用いた熱的検出カンチレバー-ESR 測定法の開発
川崎航平	M1	2014.11	日本赤外線学会 第 24 回 研究発表会	ミリ波サブミリ波領域における圧力下 ESR 測定技術の開発と応用
川崎航平	M1	2014.12	第 1 1 回強磁場フォーラム総会	圧力下強磁場高周波数 ESR 装置の開発と量子スピン系への応用
岡本翔	M1	2014.12	第 1 1 回強磁場フォーラム総会	カンチレバーを用いた溶液生体試料の高周波 ESR 測定に向けた試み
吉田翔太	M1	2014.12	第 1 1 回強磁場フォーラム総会	2次元反強磁性体 $\text{ScCu}_{2/3}\text{V}_{1/3}\text{O}_3$ の強磁場 ESR 測定
池田将平	M2	2014.12	第 1 1 回強磁場フォーラム総会	ペロブスカイト化合物 $\text{YCrO}_3$ の強磁場 ESR 測定
Alexey Alfonsov	PD	2014.12	日本物理学会大阪支部講演会	High-field electron spin resonance study of electronic inhomogeneities in correlated transition metal compounds
池田将平	M2	2014.12	若手フロンティア研究会 2014	マルチフェロイック物質 $\text{YCrO}_3$ の強磁場 ESR 測定
北原遥子	M2	2014.12	若手フロンティア研究会 2014	$S=1/2\text{NaCuMoO}_4(\text{OH})$ の強磁場 ESR 測定
岡本翔	M1	2014.12	若手フロンティア研究会 2014	カンチレバーを用いた高周波 ESR 測定法の生体試料への応用
松井亮輔	M2	2014.12	若手フロンティア研究会 2014	圧力下サイクロトロン共鳴装置の開発とディラック電子系への応用
田伏諒	M2	2014.12	若手フロンティア研究会 2014	バイメタル構造を用いたカンチレバー-ESR 測定の熱的検出法
吉田翔太	M1	2014.12	若手フロンティア研究会 2014	2次元反強磁性体 $\text{ScCu}_{2/3}\text{V}_{1/3}\text{O}_3$ のサブミリ波 ESR 測定
石川陽帆	M2	2014.12	若手フロンティア研究会 2014	カシミール力の高感度測定装置開発
荒川翔	M2	2014.12	若手フロンティア研究会 2014	巨大光学磁気電気効果を示す螺旋磁性体 $\text{CuB}_2\text{O}_4$ の ESR による研究
川崎航平	M1	2014.12	若手フロンティア研究会 2014	マイクロコイル ESR 技術の圧力下への応用
肘井敬吾	PD	2015.1	量子スピン系研究会	$S=1\text{BQ}$ 模型における付加的な $\text{SU}(2)$ 対称性とその一般化
肘井敬吾	PD	2015.3	日本物理学会 2015 年春季大会	$S=1/2$ 三量体量子スピン鎖における動的感受率の数値的研究

	北原遥子	M1	2015.3	日本物理学会 2015 年春 季大会	擬一次元フラストレート磁性体 NaCuMoO <sub>4</sub> (OH)の強磁場 ESR 測定 2
	吉田翔太	M1	2015.3	日本物理学会 2015 年春 季大会	フラストレート 2 次元反強磁性体 ScCu <sub>2/3</sub> V <sub>1/3</sub> O <sub>3</sub> の強磁場 ESR 測定
	川崎航平	M1	2015.3	日本物理学会 2015 年春 季大会	テラヘルツ領域における圧力下 ESR 装置の 開発と応用
	岡本翔	M1	2015.3	日本物理学会 2015 年春 季大会	カンチレバーを用いた高周波 ESR 測定法の 金属タンパク質への応用

**Books****著書**

著者（共著者も含む）	書名	出版社名	ページ数	発行年
秋本誠志	「葉緑体」「光化学系 I」「光化学系 II」 in: 「光化学の事典」（光化学協会編）	朝倉書店	322-327	2014

**Other Publications**
**参考論文・記事・報告**

著者	タイトル	出版物名	巻・号・ページ	発行年
Feng Zhang, Keisuke Tominaga, Michitoshi Hayashi, and Houn-Wei Wang	Low-frequency Vibration Study of Amino Acids Using Terahertz Spectroscopy and Solid-state Density Functional Theory	SPIE Proceedings Vol. 9275, "Infrared, Millimeter-Wave, and Terahertz Technologies III", Cunlin Zhang, Xi-Cheng Zhang, Masahiko Tani, Editors	Vol. 9275, 92750D-1, -9	2014
Kaoru Ohta, Kyoko Aikawa, and Keisuke Tominaga	Vibrational Dynamics of Nitrosyl Stretch of Ru Complex in Aqueous Solution Studied by Two-Dimensional Infrared Spectroscopy	"Ultrafast Phenomena XIX", edited by Kaoru Yamanouchi, Steven Cundiff, Regina de Vivie-Riedle, Makoto Kuwata-Gonokami, Louis DiMauro, Springer	pp. 479–482	2015
Sho Hiraoka, Kaoru Ohta and Keisuke Tominaga	Vibrational Dynamics of the CN Stretching in the Electronically Excited State by UV and Visible-Pump and Infrared-Probe Spectroscopy	"Ultrafast Phenomena XIX", edited by Kaoru Yamanouchi, Steven Cundiff, Regina de Vivie-Riedle, Makoto Kuwata-Gonokami, Louis DiMauro, Springer	pp. 487-491	2015
秋本誠志	生命科学を理解するための蛍光の基礎 2 (時間分解蛍光と異方性)	分光研究	63・2・73-81	2014

## Lecture to Public

## 講演、模擬授業など

氏名	講演題目	集会名	日時	場所
富永圭介	Low-frequency motions in condensed phases studied by pulsed terahertz radiation	seminar	12.15. 2014	S. N. Bose National Centre for Basic Sciences
Feng Zhang	Low-frequency Vibrations Study of Molecular Crystals Using Terahertz Spectroscopy and Solid-state Density Functional Theory	seminar at Prof. X. C. Shen's group	5.14. 2014	Shanghai Institute of Technical Physics of the Chinese Academy of Science
Feng Zhang	Low-frequency Vibrations Study of Molecular Crystals Using Terahertz Spectroscopy and Solid-state Density Functional Theory	seminar at Prof. C. L. Zhang's group	5.16.2014	Capital Normal University, China
Feng Zhang	Low-frequency Vibration Study of Molecular Solids Using Terahertz Spectroscopy and Solid-state Density Functional Theory	seminar at Prof. J. P. Wang's group	10.15. 2014	Institute of chemistry, Chinese Academy of Sciences, Beijing
Feng Zhang	Low-frequency Vibration Study of Molecular Solids Using Terahertz Spectroscopy and Solid-state Density Functional Theory	seminar at Prof. X. S. Zhao's group	10.16. 2014	Beijing University, Beijing
Feng Zhang	Low-frequency Vibration Study of Molecular Solids Using Terahertz Spectroscopy and Solid-state Density Functional Theory	seminar at Prof. Y. X. Weng's group	10.17. 2014	Institute of physics, Chinese Academy of Sciences, Beijing
太田仁	Recent development of multi-extreme high field THz ESR and some applications	Seminar	26-29.7.2014	Laboratoire National des Champs Magnetiques Intenses

## Awards

## 受賞

氏名	受賞研究題目	賞名	団体、学会名
太田仁	Fellowship	Fellowship award	International Academy of Physical Sciences
石川陽帆	Highly sensitive force detection system for high-frequency ESR measurement	SEST 学生優秀研究賞	APES2014-IES-SEST2014
川崎航平	Development of high pressure ESR system using micro-coil	SEST 学生優秀研究賞	APES2014-IES-SEST2014
岡本翔	Application of cantilever-detected ESR to biological systems	APES Poster award	APES2014-IES-SEST2014
Alexey Alfonsov	High frequency ferromagnetic resonance study of Heusler compounds using a micro-cantilever	IES Poster award	APES2014-IES-SEST2014
池田将平	マルチフェロイック物質 $\text{YCrO}_3$ の強磁場 ESR 測定	優秀賞	若手フロンティア研究会 2014

## Conference Organization

## 学術集会の開催

氏名	学術集会	共同主催者	場所	時期	参加者概数
富永圭介(代表)	Frontiers in Molecular Spectroscopy: Fundamentals and Applications to Material and Biology	Anunay Samanta (インド側代表)	奈良、東大寺総合文化センター	平成 26 年 11 月 25 日 - 28 日	約 25 名
富永圭介	先端融合科学シンポジウム「生体分子のダイナミクスを眺める」	茶谷絵理(代表)、山本直樹、鏑木基成	神戸大学理学研究科	平成 27 年 1 月 19、20 日	約 40 名
太田仁(代表)	APES-IES-SEST2014 (Joint conference of 9th Asia-Pacific EPR/ESR Society Symposium, 1st International EPR(ESR) Society Symposium, 53rd SEST Annual Meeting)	大久保晋 (Secretary General) 肘井敬吾 (Web)	奈良、東大寺総合文化センター	平成 26 年 11 月 12-16 日	289 名

### APES-IES-SEST2014



## Molecular Photoscience Seminar

## 分子フォトサイエンスセミナー

Date	Name	Affiliation	Title
7.14. 2014	Prof. Prem B. Bisht	Indian Institute of Technology Madras, Chennai	Effect of Surface Plasmon Resonances on Optical Kerr Effect in Graphene-Silver Nanoparticle Composites
7. 15. 2014	篠北啓介博士	University of Groningen	Hydrogen bond dynamics in alcohols studied by two-dimensional infrared spectroscopy
11.10.2014	御園雅俊教授	福岡大学理学部物理科学科	光周波数コムを利用した超高分解 能レーザー分光
11.4.2014	Prof. Dr. V. Kataev	IFW Dresden (分子フォトと国際協定あり)	Interplay of site disorder and magnetic frustration in the quantum spin magnet $\text{CoAl}_2\text{O}_4$
11.18.2014	Prof. Dr. K. Möbius	Free University Berlin	High-field EPR studies on biomolecules - crossing the gap to NMR
11.2014	Dr. Alexey Alfonsov	IFW Dresden, Germany (分子フォトと国際協定あり)	Multi-frequency electron spin resonance spectroscopy study of the FeAs-based superconductors
3.5.2015	Dr. Sergei Zvyagin	Dresden High Magnetic Field Laboratory	Spin dynamics in triangular-lattice antiferromagnets: high-field ESR studies

Molecular Photoscience Research Center  
Kobe University,  
Nada, Kobe 657-8501 Japan

Tel: +81-78-803-5761

URL: <http://www.kobe-u.ac.jp/mprc/index-e.html> (English)

〒657-8501  
神戸市灘区六甲台町 1-1  
神戸大学分子フォトサイエンス研究センター

電話番号 078-803-5761

URL: <http://www.kobe-u.ac.jp/mprc/> (日本語)